arXiv:1401.4792v1 [math.DS] 20 Jan 2014

Core entropy and biaccessibility of quadratic polynomials

Wolf Jung
Gesamtschule Aachen-Brand
Rombachstrasse 99, 52078 Aachen, Germany.
E-mail: jung@mndynamics.com

Abstract

For complex quadratic polynomials, the topology of the Julia set and the dynamics are understood from another perspective by considering the Hausdorff dimension of biaccessing angles and the core entropy: the topological entropy on the Hubbard tree. These quantities are related according to Thurston. Tiozzo [60] has shown continuity on principal veins of the Mandelbrot set $\mathcal{M}$. This result is extended to all veins here, and it is shown that continuity with respect to the external angle θ will imply continuity in the parameter c. Level sets of the biaccessibility dimension are described, which are related to renormalization. Hölder asymptotics at rational angles are found, confirming the Hölder exponent given by Bruin–Schleicher [11]. Partial results towards local maxima at dyadic angles are obtained as well, and a possible self-similarity of the dimension as a function of the external angle is suggested.

1 Introduction

For a real unimodal map $f(x)$, the topological entropy $h = \log\lambda$ is quantifying the complexity of iteration: e.g., the number of monotonic branches of $f^n(x)$ grows like λ^n. Moreover, $f(x)$ is semi-conjugate to a tent map of slope $\pm\lambda$; so λ is an averaged rate of expansion, which is a topological invariant [38, 42, 2]. Consider a complex quadratic polynomial $f_c(z) = z^2 + c$ with its filled Julia set $\mathcal{K}_c$, which is defined in **Section 2**:

- At least in the postcritically finite case, the interesting dynamics happens on the Hubbard tree $T_c \subset \mathcal{K}_c$: other arcs are iterated homeomorphically to T_c, which is folded over itself, producing chaotic behavior. The core entropy $h(c)$ is the topological entropy of $f_c(z)$ on T_c [1, 31, 57].
- On the other hand, for $c \neq -2$ the external angles of these arcs have measure 0, and the endpoints of $\mathcal{K}_c$ correspond to angles of full measure in the circle. This phenomenon is quantified by the Hausdorff dimension $B_{\text{top}}(c)$ of biaccessing angles: the biaccessibility dimension [63, 67, 51, 10, 36, 11].

According to Thurston, these quantities are related by $h(c) = \log 2 \cdot B_{\text{top}}(c)$, which allows to combine tools from different approaches: e.g., $B_{\text{top}}(c)$ is easily defined for every parameter c in the Mandelbrot set $\mathcal{M}$, but hard to compute explicitly. $h(c)$ is easy to compute

and to analyze when $f_c(z)$ is postcritically finite. But for some parameters c, the core may become too large by taking the closure of the connected hull of the critical orbit in $\mathcal{K}_c$.

The postcritically finite case is discussed in **Section 3**. A Markov matrix A is associated to the Hubbard tree, describing transitions between the edges. Its largest eigenvalue λ gives the core entropy $h(c) = \log\lambda$. An alternative matrix is due to Thurston [21, 22]. Or λ is obtained from matching conditions for a piecewise-linear model with constant expansion rate. This approach is more convenient for computing specific examples, but the matrix A may be easier to analyze. Known results are extended to all renormalizable maps $f_c(z)$. Here A is reducible or imprimitive, and its blocks are compared: pure satellite renormalization gives a rescaling $h(c_p * \widehat{c}) = \frac{1}{p} h(\widehat{c})$. Lower bounds of $h(c)$ for β-type Misiurewicz points and for primitive centers show that in the primitive renormalizable case, the dynamics on the small Julia sets is negligible in terms of entropy, so $h(c)$ is constant on maximal-primitive small Mandelbrot sets $\mathcal{M}_p \subset \mathcal{M}$. Moreover, it is strictly monotonic between them. An alternative proof of $h(c) = \log 2 \cdot B_{\text{top}}(c)$ shows that the external angles of T_c have finite positive Hausdorff measure.

In **Section 4**, the biaccessibility dimension is defined combinatorially for every angle $\theta \in S^1$ and topologically for every parameter $c \in \mathcal{M}$. When c belongs to the impression of the parameter ray $\mathcal{R}_M(\theta)$, we have $B_{\text{top}}(c) = B_{\text{comb}}(\theta)$ [10]. This relation means that non-landing dynamic rays have angles of negligible Hausdorff dimension, but a discussion of non-local connectivity is avoided here by generalizing results from the postcritically finite case: the biaccessibility dimension is constant on maximal-primitive Mandelbrot sets, and strictly monotonic between them. Components of a level set of positive $B_{\text{top}}(c)$ are maximal-primitive Mandelbrot sets or points. Examples of accumulation of point components are discussed. In [11, 60] the Thurston relation $h(c) = \log 2 \cdot B_{\text{top}}(c)$ was obtained for all parameters c, such that the core T_c is topologically finite. The proof extends to compact trees with infinitely many endpoints.

In an email of March 2012 quoted in [21], Thurston announced proofs of continuity for $B_{\text{comb}}(\theta)$ by Hubbard, Bruin–Schleicher, and himself. In May 2012, a proof with symbolic dynamics was given in [11], but it is currently under revision. In the present paper, it is shown that continuity of $B_{\text{comb}}(\theta)$ on S^1 will imply continuity of $B_{\text{top}}(c)$ on $\mathcal{M}$. Again, a discussion of non-local connectivity can be avoided, since the biaccessibility dimension is constant on primitive Mandelbrot sets. See version 2 of [11] for an alternative argument. Tiozzo [60] has shown that $h(c)$ and $B_{\text{top}}(c)$ are continuous on principal veins of $\mathcal{M}$; this result is extended to all veins here.

In **Section 5**, statements of Bruin–Schleicher, Zakeri, and Tiozzo [10, 11, 65, 66, 60] on the biaccessibility dimension of $\mathcal{M}$ are generalized to arbitrary pieces. In **Section 6**, Markov matrices are used again to show a geometric scaling behavior of the core entropy for specific sequences of angles, which converge to rational angles; for these examples the Hölder exponent of $B_{\text{comb}}(\theta)$ given in [11] is optimal. The asymptotics of sequences suggests the question, whether the graph of $B_{\text{comb}}(\theta)$ is self-similar; cf. the example in Figure 1. Partial results towards the Tiozzo Conjecture [60] are obtained as well, which is concerning local maxima of $B_{\text{comb}}(\theta)$ at dyadic angles. Some computations of characteristic polynomials are sketched in **Appendix A**. For the real case, statements on piecewise-linear models [38] and on the distribution of Galois conjugates [58, 59, 61] are reported in **Appendix B** to round off the discussion. See [10, 11] for the approach with symbolic dynamics and [21, 22] for the structure of critical portraits.

The present paper aims at a systematic exposition of algebraic and analytic aspects; so it contains a mixture of well-known, extended, and new results. I have tried to give proper credits and references to previous or independent work, and I apologize for possible omissions. Several people are working on reconstructing and extending Bill Thurston's results. I have been inspired by hints from or discussions with Henk Bruin, Gao Yan, Sarah Koch, Michael Mertens, Dierk Schleicher, Tan Lei, and Giulio Tiozzo.

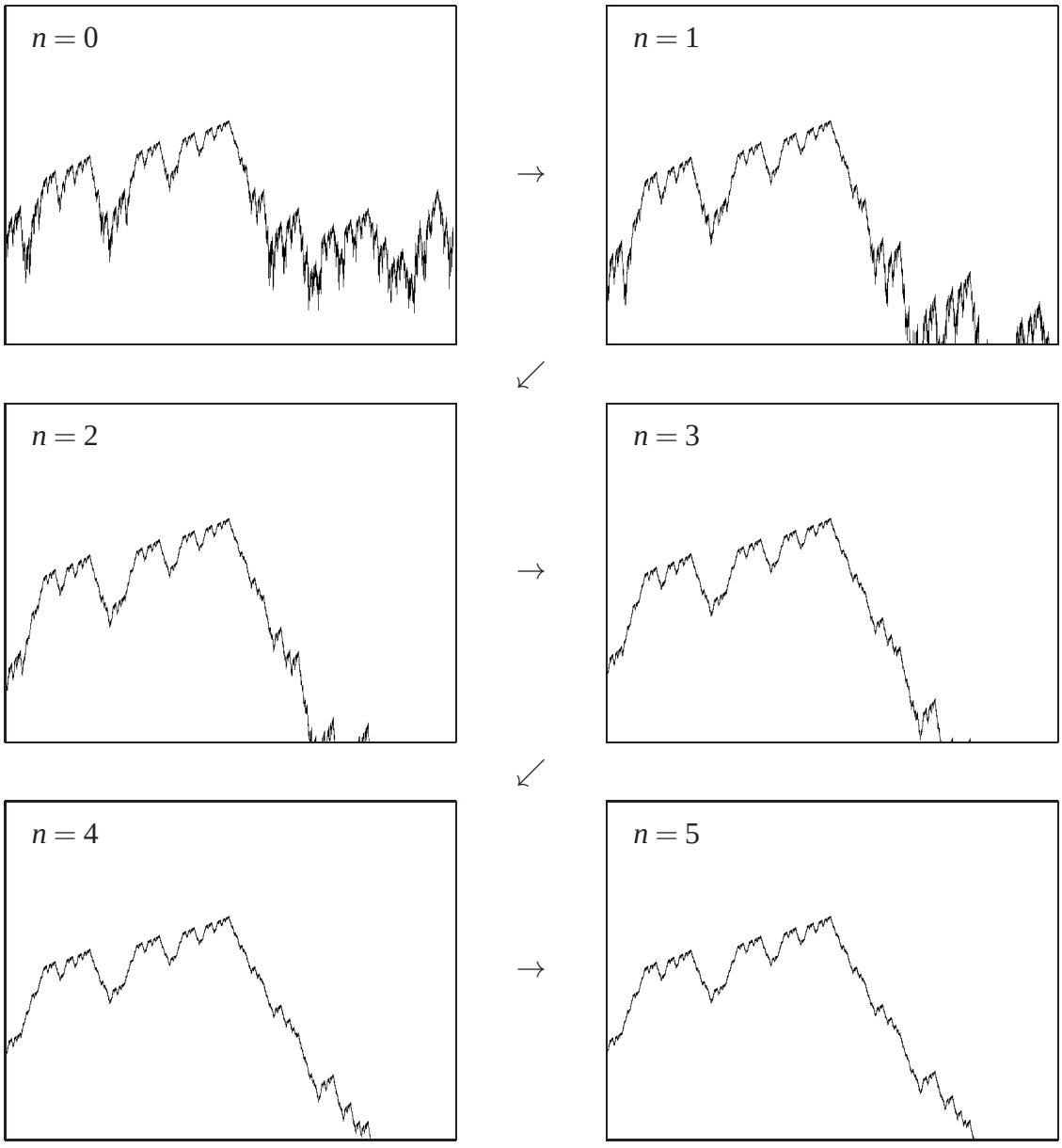

Figure 1: The biaccessibility dimension is related to the growth factor λ by $B_{\text{comb}}(\theta) = \log(\lambda(\theta))/\log 2$. Consider zooms of $\lambda(\theta)$ centered at $\theta_0 = 1/4$ with $\lambda_0 = 1.69562077$. The width is 0.201×2^{-n} and the height is $1.258 \times \lambda_0^{-n}$. There seems to be a local maximum at θ_0 and a kind of self-similarity with respect to the combined scaling by 2 and by λ_0. See Example 6.1 for the asymptotics of $B_{\text{comb}}(\theta)$ on specific sequences of angles $\theta_n \to \theta_0$.

2 Background

A short introduction to the complex dynamics of quadratic polynomials is given to fix some notations. The definitions of topological entropy and of Hausdorff dimension are recalled, and concepts for non-negative matrices are discussed.

2.1 Quadratic dynamics

Quadratic polynomials are parametrized conveniently as $f_c(z) = z^2 + c$. The filled Julia set $\mathcal{K}_c$ contains all points z with a bounded orbit under the iteration, and the Mandelbrot set $\mathcal{M}$ contains those parameters c, such that $\mathcal{K}_c$ is connected. Dynamic rays $\mathcal{R}_c(\varphi)$ are curves approaching $\partial\mathcal{K}_c$ from the exterior, having the angle $2\pi\varphi$ at ∞, such that $f_c(\mathcal{R}_c(\varphi)) = \mathcal{R}_c(2\varphi)$. They are defined as preimages of straight rays under the Böttcher map $\Phi_c : \widehat{\mathbb{C}} \setminus \mathcal{K}_c \to \widehat{\mathbb{C}} \setminus \overline{\mathbb{D}}$. Parameter rays $\mathcal{R}_M(\theta)$ approach $\partial\mathcal{M}$ [40, 49]; they are defined in terms of the Douady map $\Phi_M : \widehat{\mathbb{C}} \setminus \mathcal{M} \to \widehat{\mathbb{C}} \setminus \overline{\mathbb{D}}$ with $\Phi_M(c) := \Phi_c(c)$. The landing point is denoted by $z = \gamma_c(\varphi)$ or $c = \gamma_M(\theta)$, respectively, but the rays need not land for irrational angles, see Figure 3. There are two cases of postcritically finite dynamics:

- When the parameter c is a Misiurewicz point, the critical value $z = c$ is strictly preperiodic. Both $c \in \partial\mathcal{M}$ and $c \in \partial\mathcal{K}_c$ have the same external angles, which are preperiodic under doubling.
- When c is the center of a hyperbolic component, the critical orbit is periodic and contained in superattracting basins. The external angles of the root of the component coincide with the characteristic angles of the Fatou basin around $z = c$; the characteristic point may have more periodic angles in the satellite case.

In both cases, the Hubbard tree [16, 26] is obtained by connecting the critical orbit with regulated arcs, which are traveling through Fatou basins along internal rays. Fixing a characteristic angle θ of c, the circle $S^1 = \mathbb{R}/\mathbb{Z}$ is partitioned by the diameter joining $\theta/2$ and $(\theta+1)/2$ and the orbit of an angle $\varphi \in S^1$ under doubling is encoded by a sequence of symbols $A, B, *$ or $1, 0, *$. There is a corresponding partition of the filled Julia set, so points $z \in \mathcal{K}_c$ are described by symbolic dynamics as well. The kneading sequence is the itinerary of θ or of c, see [26, 49, 10].

$\mathcal{M}$ consists of the closed main cardioid and its limbs, which are labeled by the rotation number at the fixed point α_c; the other fixed point β_c is an endpoint of $\mathcal{K}_c$. A partial order on $\mathcal{M}$ is defined such that $c \prec c'$ when c' is disconnected from 0 in $\mathcal{M} \setminus \{c\}$. See Sections 3.3 and 4.1 for the notion of renormalization [14, 15, 25, 39, 48, 28], which is explaining small Julia sets within Julia sets and small Mandelbrot sets within the Mandelbrot set. Primitive and satellite renormalization may be nested; a primitive small Mandelbrot set will be called maximal-primitive, if it is not contained in another primitive one. A pure satellite is attached to the main cardioid by a series of satellite bifurcations, so it is not contained in a primitive Mandelbrot set.

2.2 Topological entropy

Suppose X is a compact metric space and $f : X \to X$ is continuous. The topological entropy is measuring the complexity of iteration from the growth rate of the number of

distinguishable orbits. The first definition assumes an open cover U and considers the minimal cardinality $V_U(n)$ of a subcover, such that all points in a set of the subcover have the same itinerary with respect to U for n steps. See, e.g., [17, 31]. The second definition is using the minimal number $V_\varepsilon(n)$ of points, such that every orbit is ε-shadowed by one of these points for n steps [8, 37]. We have

$$h_{\text{top}}(f,X) := \sup_U \lim_{n\to\infty} \frac{1}{n} \log V_U(n) = \lim_{\varepsilon\to 0} \limsup_{n\to\infty} \frac{1}{n} \log V_\varepsilon(n) \; . \tag{1}$$

For a continuous, piecewise-monotonic interval map, the growth rate of monotonic branches (laps) may be used instead, or the maximal growth rate of preimages [42, 17]. The same result applies to endomorphisms of a finite tree [2, 31]. Moreover, f is semi-conjugate to a piecewise-linear model of constant expansion rate λ when $h_{\text{top}}(f,X) = \log\lambda > 0$; this is shown in [38, 17, 2] for interval maps and in [4] for tree maps. See Section B for the relation to the kneading determinant and Section 4.4 for continuity results [38, 42, 43, 17, 2]. If $\pi : X \to Y$ is a surjective semi-conjugation from $f : X \to X$ to $g : Y \to Y$, then $h_{\text{top}}(g,Y) \le h_{\text{top}}(f,X)$. Equality follows when every fiber is finite, but fiber cardinality need not be bounded globally [8, 37].

2.3 Hausdorff dimension

The d-dimensional Hausdorff measure is a Borel outer measure. It is defined as follows for a bounded subset $X \subset \mathbb{R}$ or a subset $X \subset S^1 = \mathbb{R}/\mathbb{Z}$:

$$\mu_d(X) := \lim_{\varepsilon\to 0} \inf_U \sum_i |U_i|^d \tag{2}$$

Here the cover U of X is a countable family of intervals U_i of length $|U_i| \le \varepsilon$. They may be assumed to be open or closed, aligned to nested grids or not, but the important point is that they may be of different size. When an interval is replaced with two subintervals, the sum may grow in fact when $d < 1$. In general, the Hausdorff measure of X may be easy to bound from above by using intervals of the same size, but it will be hard to bound from below, since this requires to find an optimal cover with intervals of different sizes.

The Hausdorff dimension $\dim(X)$ is the unique number in $[0,1]$, such that $\mu_d(X) = \infty$ for $0 \le d < \dim(X)$ and $\mu_d(X) = 0$ for $\dim(X) < d \le 1$. For $d = \dim(X)$, the Hausdorff measure $\mu_d(X)$ may be 0, positive and finite, or ∞. The Hausdorff dimension of a countable set is 0 and the dimension of a countable union is the supremum of the dimensions. Again, $\dim(X)$ may be easy to bound from above by the box dimension, which corresponds to equidistant covers, but it is harder to bound from below. Sometimes this is achieved by constructing a suitable mass distribution according to the Frostman Lemma [19, 65]. When $X \subset S^1$ is closed and invariant under doubling $F(\varphi) = 2\varphi$, the Hausdorff dimension $\dim(X)$ is equal to the box dimension according to Furstenberg [20].

2.4 Perron–Frobenius theory

The Perron theory of matrices with positive elements was extended by Frobenius to non-negative matrices, see [24]. We shall need the following features of a square matrix $A \ge 0$:

- There is a non-negative eigenvalue λ with non-negative eigenvector, such that all eigenvalues of A are $\leq \lambda$ in modulus. λ is bounded above by the maximal sum of rows or columns, and bounded below by the minimal sum.

- $A \geq 0$ is called reducible, if it is conjugate to a block-triangular matrix by a permutation. It is irreducible (ergodic) if the corresponding directed graph is strongly connected. Then λ is positive and it is an algebraically simple eigenvalue. The eigenvector of λ is positive, and other eigenvectors are not non-negative.

- An irreducible $A \geq 0$ is called primitive (mixing), if the other eigenvalues have modulus $< \lambda$. Equivalently, $A^n > 0$ element-wise for some n.

- If A is irreducible but imprimitive with $p > 1$ eigenvalues of modulus λ, its characteristic polynomial is of the form $x^k P(x^p)$. The Frobenius normal form shows that there are p subspaces mapped cyclically by A.

- If $B \geq A$ element-wise with $B \neq A$ and A is primitive, then $\lambda_B > \lambda_A$. This is proved by choosing n with $A^n > 0$, noting $B^n \geq A^n$, so B^{n+1} is strictly larger than A^{n+1} in at least one row and one column, and finally $B^{2n+1} > A^{2n+1}$. Now fix $\varepsilon > 0$ with $B^{2n+1} \geq (1+\varepsilon)A^{2n+1}$ and consider higher powers to show $\lambda_B \geq \sqrt[2n+1]{1+\varepsilon}\,\lambda_A$.

To obtain λ numerically from $A \geq 0$, we do not need to determine the characteristic polynomial and its roots: for some positive vector v_0 compute $v_n = A^n v_0$ recursively, then $\lambda = \lim \sqrt[n]{\|v_n\|}$ converges slowly. If A is irreducible and primitive, $\lambda = \lim \|v_{n+1}\| / \|v_n\|$ will converge exponentially fast.

3 Postcritically finite polynomials and core entropy

Suppose $f_c(z)$ is postcritically finite and consider the Hubbard tree T_c. Since the collection of vertices is forward invariant, each edge is mapped to one edge or to several adjacent edges. Thus the edges form a Markov partition (strictly speaking, a tessellation). By numbering the edges, the map is described by a non-negative matrix A with entries 0 and 1, such that the j-th column is showing where the j-th edge of T_c is mapped by $f_c(z)$. The Markov matrix A is the transition matrix of the Markov partition and the adjacency matrix of the Markov diagram. Often the transposed matrix is used instead. In the preperiodic case, no postcritical point is mapped to the critical point $z = 0$. So we still have a Markov partition when the two edges at 0 are considered as one edge, but mapping this edge will cover the edge before $z = c$ twice, resulting in an entry of 2 in A.

Definition 3.1 (Markov matrix and core entropy)
For a postcritically finite quadratic polynomial $f_c(z)$, the Markov matrix A is the transition matrix for the edges of the Hubbard tree T_c. Its highest eigenvalue λ gives the core entropy $h(c) := \log \lambda$. Equivalently, $h(c) := h_{\text{top}}(f_c, T_c)$ is the topological entropy on T_c.

The i-th row of A says which edges are mapped to an arc covering the i-th edge. Since $f_c : T_c \to T_c$ is surjective and at most 2:1, the sum of each row of A is 1 or 2, so the highest eigenvalue of A satisfies $1 \leq \lambda \leq 2$. The largest entries of A^n are growing as $\asymp \lambda^n$ when $\lambda > 1$. (Not as $n^k \lambda^n$: according to Section 3.3, A may be reducible but $\lambda > 1$ corresponds to a unique irreducible block, which need not be primitive.) Since the entries of A^n give

the number of preimages of edges, the same estimate applies to the maximal cardinality of preimages $f_c^{-n}(z_0)$ in T_c. There are various ways to show that $\log\lambda$ is the topological entropy of $f_c(z)$ on the Hubbard tree T_c:

- By expansivity, every edge is iterated to an edge at $z=0$, so the preimages of 0 are growing by λ^n even if the edges at 0 correspond to an irreducible block of lower eigenvalues. So the number of monotonic branches of $f_c^n(z)$ is growing by the same rate, which determines the topological entropy according to [2].

- This criterion is obtained from the definition according to Section 2.2 by showing that the open cover may be replaced with closed arcs having common endpoints, and that the maximal growth rate is attained already for the given edges [17, 31].

- According to [4], $f_c(z)$ on T_c is semi-conjugate to a piecewise-linear model with constant expansion rate λ when the topological entropy is $\log\lambda > 0$. See also [38, 17] for real parameters and [60] for parameters on veins. Now the highest eigenvector of the transposed matrix A' is assigning a Markov length to the edges, such that $f_c(z)$ corresponds to multiplying the length with λ. Note that according to the decomposition (3) in Section 3.3, the edges in a primitive small Julia set have Markov length 0 and will be squeezed to points by the semi-conjugation.

3.1 Computing the core entropy

Let us start with four examples of postcritically finite parameters c in the $1/3$-limb of $\mathcal{M}$. The external angle $\theta = 3/15$ gives a primitive center of period 4. The other examples are preperiodic and the edges at $z=0$ are united. $\theta = 1/4$ defines a β-type Misiurewicz point of preperiod 2 and $\theta = 9/56$ gives an α-type Misiurewicz point of preperiod 3 and ray period 3; it is satellite renormalizable of period 3 and the Markov matrix A is imprimitive of index 3. And $\theta = 1/6$ gives $c = \mathrm{i}$, a Misiurewicz point with preperiod 1 and period 2.

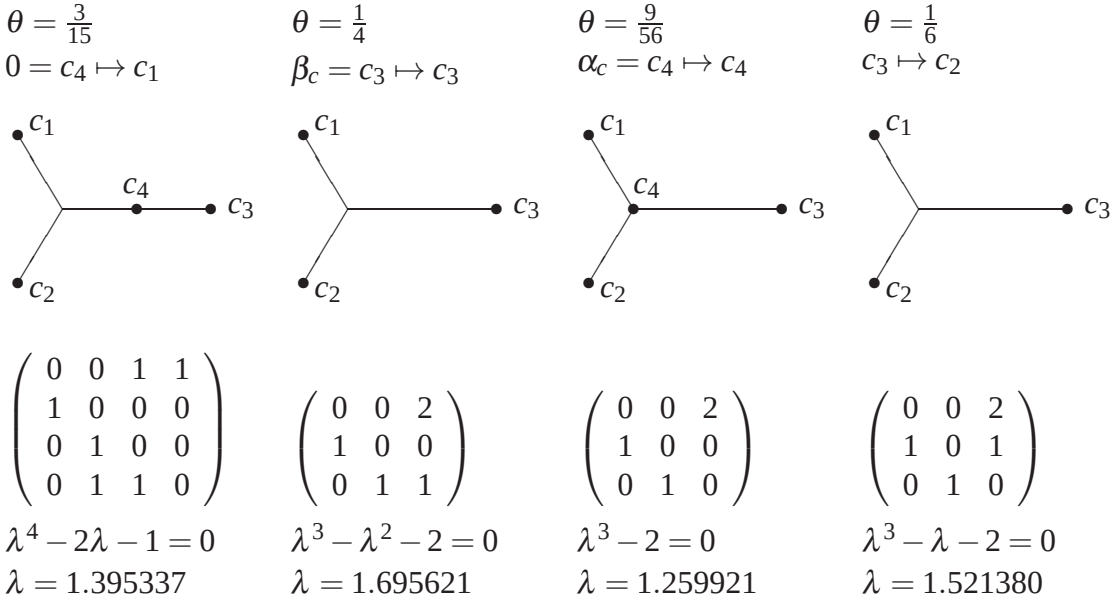

Figure 2: Examples of Hubbard trees and Markov matrices defined by an angle θ. Here $f_c(z)$ maps $c = c_1 \mapsto c_2 \mapsto c_3 \mapsto c_4$ and the edges are numbered such that the first edge is before $c_1 = c$.

Instead of computing the characteristic polynomial of the Markov matrix A, we may use a piecewise-linear model with expansion constant $\lambda > 1$ to be matched: in Figure 2, the edges or arcs from α_c to c_1, c_2, c_3 have length λ, λ^2, λ^3 when $[0, \pm\alpha_c]$ has length 1.
For $\theta = 3/15$, we have $[-\alpha_c, c_3] \mapsto [\alpha_c, c_4]$, so $\lambda(\lambda^3 - 2) = 1$.
For $\theta = 1/4$, we have $[-\alpha_c, c_3] \mapsto [\alpha_c, c_3]$, so $\lambda(\lambda^3 - 2) = \lambda^3$.
For $\theta = 9/56$, we have $c_3 = -\alpha_c$, so $\lambda^3 = 2$.
For $\theta = 1/6$, we have $[-\alpha_c, c_3] \mapsto [\alpha_c, c_2]$, so $\lambda(\lambda^3 - 2) = \lambda^2$.

Example 3.2 (Lowest periods and preperiods in limbs)
The p/q-limb of $\mathscr{M}$ contains those parameters c, such that the fixed point α_c has the rotation number p/q. The principal vein is the arc from 0 to the β-type Misiurewicz point of preperiod $q-1$. The examples in Figure 2 can be generalized by considering sequences of Markov matrices or by replacing $\lambda^3 - 2$ with $\lambda^q - 2$ for the piecewise-linear models. This gives the following polynomials for λ:
β-type Misiurewicz point of preperiod $q-1$: $x^q - x^{q-1} - 2 = 0$ [1]
Primitive center of period $q+1$: $x^{q+1} - 2x - 1 = 0$
α-type Misiurewicz point of preperiod q: $x^q = 2$
These equations show that $h(c)$ is not Hölder continuous with respect to the external angle θ as $\theta \to 0$, see Section 4.5.

Example 3.3 (Sequences on principal veins)
On the principal vein of the p/q-limb, the β-type Misiurewicz point is approached by a sequence of centers c_n and α-type Misiurewicz points a_n of increasing periods and preperiods. The corresponding polynomials for λ_n are obtained from piecewise-linear models again, or by considering a sequence of matrices. The polynomial is simplified by summing a geometric series and multiplying with $\lambda - 1$:
Center c_n of period $n \geq q+1$: $x^{n+1} - x^n - 2x^{n+1-q} + x + 1 = 0$
α-type Misiurewicz point a_n of preperiod $n \geq q$: $x^{n+1} - x^n - 2x^{n+1-q} + 2 = 0$
These polynomials imply monotonicity of λ_n and give geometric asymptotics by writing $x^{n+1} - x^n - 2x^{n+1-q} = x^{n+1-q} \cdot (x^q - x^{q-1} - 2)$; note that the largest root λ_0 of the latter polynomial corresponds to the endpoint of the vein according to Example 3.2:
For c_n we have $\lambda_n \sim \lambda_0 - K_c \cdot \lambda_0^{-n}$ with $K_c = \frac{\lambda_0 + 1}{q - (q-1)/\lambda_0} > 0$.
For a_n we have $\lambda_n \sim \lambda_0 - K_a \cdot \lambda_0^{-n}$ with $K_a = \frac{2}{q - (q-1)/\lambda_0} > 0$.
See Proposition 6.2 and Appendix A for a detailed computation and Remark 6.4 for the relation to Hölder continuity.

Example 3.4 (Sequences on the real axis)
The real axis is the principal vein of the $1/2$-limb; setting $q = 2$ in Example 3.3, dividing by $\lambda + 1$ and noting $\lambda_0 = 2$ at the endpoint $c = -2$ gives:
c_n of period $n \geq 3$: $x^n - 2x^{n-1} + 1 = 0$, $\lambda_n \sim 2 - 2 \cdot 2^{-n}$
a_n of preperiod $n \geq 2$: $x^{n+1} - x^n - 2x^{n-1} + 2 = 0$, $\lambda_n \sim 2 - \frac{4}{3} \cdot 2^{-n}$
Now consider the α-type Misiurewicz point a_2 with the external angle $\theta = 5/12$ and with $\lambda_a = \sqrt{2}$, which is the tip of the satellite Mandelbrot set of period 2. It is approached from above (with respect to $\prec$, i.e., from the left) by centers c'_n of periods $n = 3, 5, 7, \ldots$ related to the Šharkovskiĭ ordering. The entropy was computed by Štefan [54], and the centers of even periods before a_2 (to the right) are treated analogously. Again, geometric asymptotics are obtained from the sequence of polynomials for λ'_n:
c'_n of period $n = 3, 5, 7, \ldots$: $x^n - 2x^{n-2} - 1 = 0$, $\lambda'_n \sim \lambda_a + \frac{1}{\sqrt{2}} \cdot \lambda_a^{-n}$

c'_n of period $n = 4, 6, 8, \ldots$: $x^n - 2x^{n-2} + 1 = 0$, $\lambda'_n \sim \lambda_a - \frac{1}{\sqrt{2}} \cdot \lambda_a^{-n}$
Note that for even periods n, the polynomial for λ'_n is imprimitive of index 2, which is related to the satellite renormalization according to Section 3.3.

Constructing the Hubbard tree T_c from an external angle θ is quite involved [10]. In [21, 22] an alternative matrix F by Thurston is described, which is obtained from an external angle without employing the Hubbard tree. Actually, only the kneading sequence of the angle is required to determine F from the parts of $T_c \setminus \{0\}$:

Proposition 3.5 (Alternative matrix by Thurston and Gao)
From a rational angle or from a $*$-periodic or preperiodic kneading sequence, construct a transition matrix F. The basic vectors represent non-oriented arcs between postcritical points $c_j = f_c^j(0)$, $j \geq 1$, and $[c_j, c_k]$ is mapped to $[c_{j+1}, c_{k+1}]$ by F unless its endpoints are in different parts of $\mathcal{K}_c \setminus \{0\}$: then it is mapped to $[c_1, c_{j+1}] + [c_1, c_{k+1}]$.
Now the largest eigenvalues of the Thurston matrix F and the Markov matrix A coincide.

This combinatorial definition corresponds to the fact that an arc covering $z = 0$ is mapped 2:1 to an arc at $z = c$ by $f_c(z)$. Arcs at c_0 are omitted in the preperiodic case, because they would generate a diagonal 0-block anyway. Note that in general F is considerably larger than A; it will contain large nilpotent blocks and it may contain additional blocks, which seem to be cyclic. In the case of β-type Misiurewicz points, a small irreducible block of F is obtained in Proposition 3.8.3.

Proof: Gao [22] is using a non-square incidence matrix C, which is mapping each arc to a sum of edges, so $AC = CF$. Consider the non-negative Frobenius eigenvectors to obtain equality of the highest eigenvalues: if $Fy = \lambda_F y$ then Cy is an eigenvector of A with eigenvalue λ_F. The transposed matrices satisfy $F'C' = C'A'$ and if $A'x = \lambda_A x$, then $C'x$ is an eigenvector of F' with eigenvalue λ_A. (Note that Cy and $C'x$ are not 0, because C has a non-zero entry in each row and each column.)

As an alternative argument, define a topological space X_c as a union of arcs $[c_j, c_k] \subset \mathcal{K}_c$, which are considered to be disjoint except for common endpoints. There is a natural projection $\pi_c : X_c \to T_c$ and a lift $F_c : X_c \to X_c$ of $f_c(z)$, such that π_c is a semi-conjugation and F is the transition matrix of F_c. Now any $z \in T_c$ has a finite fiber $\pi_c^{-1}(z) = \{x_i\} \subset X_c$ and we have the disjoint union $\bigcup F_c^{-n}(x_i) = \pi_c^{-1}(f_c^{-n}(z))$. Choosing z such that the cardinality of $f_c^{-n}(z)$ is growing by λ_A^n shows $\lambda_A \leq \lambda_F$. And choosing z such that the cardinality of $F_c^{-n}(x_1)$ is growing by λ_F^n gives $\lambda_F \leq \lambda_A$.

Note that F is determined from the kneading sequence of $c_1 = c$, which can be obtained from the external angle θ as an itinerary. Alternatively, consider a matrix where the basic vectors represent pairs of angles $\{2^{j-1}\theta, 2^{k-1}\theta\}$; it will be the same as F except in the preperiodic satellite case, where c_1 is entering a repelling p-cycle of ray period $rp > p$. (This cycle contains the characteristic point of a satellite component before the Misiurewicz point c.) The matrix of transitions between pairs of angles will be different from F, but the largest eigenvalue will be the same: pairs of equivalent angles are permuted cyclically and correspond to eigenvalues of modulus 1 [22]. Arcs of X_c with at least one p-periodic endpoint are represented by several pairs of angles, but when a topological space is built from multiple copies of arcs, it comes with a semi-conjugation to X_c or to T_c again. ■

3.2 Estimates of the core entropy

The edges of the Hubbard tree are connecting the marked points: the critical orbit $f_c^n(0)$, $n \geq 0$, which includes all endpoints, and additional branch points.

Lemma 3.6 (Modified Markov matrix)
For a postcritically finite $f_c(z)$, the Hubbard tree T_c and the associated Markov matrix A may be changed as follows, without changing the highest eigenvalue λ, and without changing irreducibility or primitivity (except for item 4 and for $c = -1$ in item 2):

1. *If c is preperiodic, the two edges at $z = 0$ may be considered as one edge by removing $z = 0$ from the marked points; thus an eigenvalue 0 has been removed from A.*
2. *For c in the $1/2$-limb, the unmarked fixed point α_c may be marked, splitting one edge in two. This gives an additional eigenvalue of -1.*
3. *An unmarked preimage of a marked periodic or preperiodic point may be marked.*
4. *Extend the Hubbard tree T_c by attaching edges towards the fixed point β_c and/or some of its preimages. This gives additional eigenvalues of 1 and 0, and it makes A reducible.*

These modifications may be combined, and item 3 can be applied recursively. The **proof** is deferred to Appendix A. Figure 2 gives examples of item 1. Items 2 and 3 are applied in Section 3.3. Item 4 shows that for a biaccessible parameter c, the Hubbard tree T_c may be extended in a uniform way for all parameters on the vein. E.g., in the real case we may replace $T_c = [c,\, f_c(c)]$ with $[-\beta_c\,, \beta_c]$. Item 4 is used as well to prove Proposition 6.6. Note that a matrix with an eigenvalue 0, -1, or 1 will be reduced by a conjugation in $GL(\mathbb{Q}^N)$, but only permutations are considered for a Frobenius irreducible matrix.

Proposition 3.7 (Monotonicity of core entropy, Penrose and Tao Li)
Core entropy is monotonic: for postcritically finite $c \prec c'$ we have $h(c) \leq h(c')$.

Not all parameters are comparable with the partial order $\prec$. In particular, many parameters c' are approached by branch points c before them, and parameters c'' in different branches are not comparable to c'. — The proof below employs Hubbard trees. Tao Li [31] used the semi-conjugation from the angle doubling map, see Section 4.2. Penrose had obtained a more general statement for kneading sequences [44]. See also Proposition 4.6 for monotonicity with respect to external angles.

Proof: The periodic and preperiodic points marked in the Hubbard tree T_c of $f_c(z)$ move holomorphically for parameters in the wake of c. The Hubbard tree $T_{c'}$ contains the characteristic point $z_{c'}$ corresponding to c and the connected hull $T \subset T_{c'}$ of its orbit is homeomorphic to T_c, but the dynamics of $f_{c'}(z)$ is different in a neighborhood of $z = 0$, which is mapped behind the characteristic point. There is a forward-invariant Cantor set $C \subset T$ defined by removing preimages of that neighborhood. To obtain the lower estimate of $h(c')$, either note that the preimages of a suitable point in C under $f_{c'}(z)$ correspond to those in T_c under $f_c(z)$, or consider a semi-conjugation π from $C \subset T_{c'}$ to T_c. If c is a center, hyperbolic arcs in T_c must be collapsed first. ∎

A parameter $c \in \mathcal{M}$ is a β-type Misiurewicz point, if $f_c^k(c) = \beta_c$; the minimal $k \geq 1$ is the preperiod. The following results will be needed for Proposition 3.11. The weaker estimate $h(c) \geq \frac{\log 2}{k+1}$ is obtained from Corollary E in [1]; it does not give Proposition 3.11.2.

Proposition 3.8 (β-type Misiurewicz points)
Suppose c is a β-type Misiurewicz point of preperiod $k \geq 1$.

1. *The Markov matrix A is irreducible and primitive.*

2. *The largest eigenvalue satisfies $\lambda^k \geq 2$, so $h(c) \geq \frac{\log 2}{k}$, with strict inequality for $k \geq 2$.*

3. *For the Thurston matrix F according to Proposition 3.5, the arc $[c, \beta_c]$ is generating an irreducible primitive block B of F, which corresponds to the largest eigenvalue λ.*

Proof: Consider the claim that the union $\bigcup f_c^j([0, \beta_c])$, $1 \leq j \leq k$, gives the complete Hubbard tree T_c: we have $f_c^1([-\alpha_c, \beta_c]) = [\alpha_c, \beta_c]$ and $f_c^j([0, -\alpha_c])$, $1 \leq j \leq k$, provides arcs from α_c to all endpoints except β_c. When an arc from α_c is crossing $z = 0$, then either its endpoint is behind $-\alpha_c$ and the part before $-\alpha_c$ is chopped away before the next iteration. Or this arc is branching off between 0 and $-\alpha_c$, and further iterates will be branching from arcs at α_c constructed earlier. This proves the claim.

2. Now the arc $[0, \beta_c]$ is containing preimages of itself, so $f_c^k([0, \beta_c])$ is the Hubbard tree T_c. Since $f_c^k(z)$ is even, every arc of the Hubbard tree has at least two preimages under $f_c^k(z)$ on the spine $[-\beta_c, \beta_c] \subset T_c$. Each row of A^k has a sum ≥ 2, so $\lambda^k \geq 2$.

1. Every edge e of T_c covers $z = 0$ in finitely many iterations. Then it is iterated to an arc at β_c, so the edge e contains an arc iterated to $[0, \beta_c]$. Now $f_c^n(e) = T_c$ for $n \geq n_e$, and A^n is strictly positive for $n \geq \max\{n_e \,|\, e \subset T_c\}$, thus A is irreducible and primitive. (Alternatively, this follows from Lemma 3.9.4, since f_c is not renormalizable.) Finally, if $k \geq 2$ and we had $\lambda^k = 2$, the characteristic polynomial of A would contain the irreducible factor $x^k - 2$ and A would be imprimitive.

3. Denote the postcritical points by $c_j = f_c^{j-1}(c)$ again. The iteration of any arc is giving two image arcs frequently, but at least one of these has an endpoint with index j growing steadily, so reaching $\beta_c = c_{k+1}$. Further iterations produce the arc $[c, \beta_c]$ after the other endpoint was in part A of $\mathcal{K}_c \setminus \{0\}$, which happens when it becomes $-\beta_c$ or earlier. So the forward-invariant subspace generated by $[c, \beta_c]$ corresponds to an irreducible block B of F. It is primitive by the same arguments as above, since $[c, \beta_c] \mapsto [c, \beta_c] + [c, c_2]$. Consider the lift $F_c : X_c \to X_c$ from the proof of Proposition 3.5 and the invariant subset X_c' corresponding to B. Now $\pi_c : X_c' \to T_c$ is surjective, since it maps $[c, \beta_c] \subset X_c'$ to $[c, \beta_c] \subset T_c$, and we have $\lambda_B = \lambda_A$ again. Certainly this block B of F need not be equivalent to A: for $\theta = 3/16$, A is 7×7 and B is 6×6. And for $\theta = 3/32$, A is 8×8 and B is 9×9. ■

3.3 Renormalization

A filled Julia set $\mathcal{K}_c$ may contain a copy $\mathcal{K}_c^p$ of another Julia set $\mathcal{K}_{\widehat{c}}$, and the Mandelbrot set $\mathcal{M}$ contains a corresponding copy $\mathcal{M}_p$ of itself. According to Douady and Hubbard, this phenomenon is explained by renormalization: in a suitable neighborhood of $\mathcal{K}_c^p$, the iterate $f_c^p(z)$ is quasi-conformally conjugate to $f_{\widehat{c}}(\widehat{z})$. See [14, 15, 25, 39, 48]. Many basic results are hard to find in the literature; a self-contained exposition will be given in [28].

For a primitive or satellite center c_p of period p there is a corresponding tuning map $\mathcal{M} \to \mathcal{M}_p$, $\widehat{c} \mapsto c = c_p * \widehat{c}$. This notation suggests that the centers are acting on $\mathcal{M}$ as a semigroup. Primitive and satellite renormalization are referred to as simple renormalization, in contrast to crossed renormalization [35, 45, 39]. A small Mandelbrot set $\mathcal{M}_p$ is maximal, if it is not contained in another small Mandelbrot set; then it is either

primitive maximal or generated by a satellite of the main cardioid. We shall need two non-standard notations: a *pure satellite component* is not contained in a primitive Mandelbrot set, but attached to the main cardioid with a series of satellite bifurcations. And a *maximal-primitive* small Mandelbrot set is not contained in another primitive one, but it may be either maximal and primitive or contained in a pure satellite Mandelbrot set.

If c_p is primitive and $\widehat{c}$ is postcritically finite, the Hubbard tree for $c = c_p * \widehat{c}$ is understood in this way: visualize the p-periodic marked points in the Hubbard tree of c_p as small disks, which are mapped to the next one 1:1 or 2:1, and replace each disk with a copy of the Hubbard tree of $\widehat{c}$. Actually, the latter Hubbard tree is extended to include $\pm\beta_{\widehat{c}}$. The Markov matrix is obtained in block form as follows, where I denotes an identity matrix:

$$A = \left(\begin{array}{c|c} B & 0 \\ \hline X & R \end{array}\right) \qquad \text{with} \qquad R = \begin{pmatrix} 0 & 0 & 0 & \cdots & \widehat{A} \\ \mathrm{I} & 0 & 0 & \ddots & 0 \\ 0 & \mathrm{I} & 0 & \ddots & 0 \\ \vdots & \ddots & \ddots & \ddots & 0 \\ 0 & 0 & 0 & \mathrm{I} & 0 \end{pmatrix} \tag{3}$$

Lemma 3.9 (Renormalization and Markov matrices)
1. *Suppose $c = c_p * \widehat{c}$ for a postcritically finite parameter $\widehat{c} \neq 0$. In particular, c_p is a center of period $p \geq 2$ and a suitable restriction of $f_c^p(z)$ is conjugate to $f_{\widehat{c}}(\widehat{z})$. Then the edges of the Hubbard tree can be labeled such that the Markov matrix A has the block form (3). Here R is imprimitive and $\widehat{A}$ is the Markov matrix of $\widehat{c}$. Moreover:*
a) If c_p is a primitive center or $\widehat{c}$ is not a β-type Misiurewicz point, then B is the Markov matrix of c_p.
b) If c_p is a satellite of c_p' and $\widehat{c}$ is of β-type, then B belongs to c_p'. It is missing completely for immediate satellite renormalization with $c_p' = 0$.

2. *In all cases of simple renormalization, we have $h(c) = \max\left\{h(c_p)\,,\, \frac{1}{p}\,h(\widehat{c})\right\}$.*

3. *Suppose $f_c(z)$ is crossed renormalizable of immediate type and a suitable restriction of $f_c^p(z)$ is conjugate to $f_{\widehat{c}}(\widehat{z})$. Then its Markov matrix A is imprimitive and it can be given the form $A = R$ from (3). Here $\widehat{A}$ is the Markov matrix of $\widehat{c}$, with $\alpha_{\widehat{c}}$ added to the marked points if necessary, so $h(c) = \frac{1}{p}\,h(\widehat{c})$.*

4. *If the Markov matrix A of $f_c(z)$ is reducible or imprimitive, then $f_c(z)$ is simply or crossed renormalizable with $\widehat{c} \neq 0$, or c is an immediate satellite center.*

In the preperiodic case, $f_c(z)$ is topologically transitive on the Hubbard tree T_c, if A is irreducible, and total transitivity corresponds to a primitive matrix. In this context, results similar to items 1 and 4 have been obtained in [1]. However, it is assumed that the small Hubbard trees are disjoint only in the case of primitive renormalization. But $f_c(z)$ is not transitive in the pure satellite case either, except in the immediate satellite case with $\widehat{c}$ of β-type. — In real dynamics, the relation of imprimitivity and renormalization is classic. Item 2 is found in [38, 17] for real unimodal maps, in [31] for postcritically finite complex polynomials, and in [60] for arbitrary parameters on veins.

Proof of Lemma 3.9: Note that for $c = c_p$ and $\widehat{c} = 0$, the map $f_c(z)$ is p-renormalizable as well, but the small Hubbard tree is reduced to a point and R is empty. On the other hand, items 1–3 do not require p to be the maximal non-trivial renormalization period. Likewise, the proof of item 4 will not produce that period in general.

1. The Julia set of $f_{c_p}(z)$ contains both a superattracting orbit of period p and a characteristic point of period dividing p. By tuning, the superattracting basins are replaced with a p-cycle of small Julia sets, which are attached to the characteristic point and its images. These sets are mapped homeomorphically to the next one; only the small Julia set at $z=0$ is mapped 2:1 to the set at $z=c$. The I-blocks in R represent the homeomorphic restrictions of $f_c^1(z)$, and the diagonal block $\widehat{A}$ in R^p corresponds to $f_c^p(z)$ and $f_{\widehat{c}}(\widehat{z})$. Except in the β-type case of $\widehat{c}$, the edges of the Hubbard tree for $f_{c_p}(z)$ are extended into the small Julia sets, ending at marked points of the small Hubbard trees, which are before those corresponding $\pm\beta_{\widehat{c}}$. This extension does not happen in the case of a β-type Misiurewicz point $\widehat{c}$, because the β-fixed point of the small Hubbard tree coincides with the characteristic point corresponding to c_p. In the satellite case, this means that the edges from the characteristic point to the p-periodic points are lost completely; only edges from the Hubbard tree of c'_p are represented in B. Note that in the preperiodic case, we must join the edges at $z=0$ according to Lemma 3.6.1; otherwise the block R will be more involved.

2. The characteristic polynomials satisfy $\chi_A(x)=\chi_B(x)\cdot\chi_R(x)=\chi_B(x)\cdot\chi_{\widehat{A}}(x^p)$. For the second equality, consider a complex eigenvector in block form to see that x is an eigenvalue of R if and only if x^p is an eigenvalue of $\widehat{A}$. Now the largest eigenvalue of B is related to $h(c_p)$ and the largest eigenvalue of R corresponds to $\frac{1}{p}h(\widehat{c})$. When B represents c'_p instead of c_p, first apply the same argument to show $h(c'_p)=h(c_p)$.

3. The p-cycle of small Julia sets is mapped $p-1$ times homeomorphically and once like $f_c^p(z)$ and $f_{\widehat{c}}(\widehat{z})$ as above. Since they are crossing at the fixed point α_c, $\alpha_{\widehat{c}}$ is marked in the Hubbard tree determining the block $\widehat{A}$. If $\widehat{c}$ belongs to the $1/2$-limb and is not of α-type, this point would not be marked in the minimal Hubbard tree of $f_{\widehat{c}}(\widehat{z})$, but doing so does not change the largest eigenvalue according to Lemma 3.6.2. There are no further edges in the Hubbard tree of $f_c(z)$.

4. Since $f_c(z)$ is expanding on the Hubbard tree T_c, every edge will cover the edge e_c before $z=c$ under the iteration. So the images $f_c^j(e_c)$ form an absorbing invariant family of edges, and there is a corresponding irreducible block R in A. If A is reducible, R is not all of A, and the corresponding subset of T_c has $p\geq 2$ connected components: if it was connected, it would be all of T_c. By surjectivity, each of these components is mapped onto another one. Each component is forming a small tree, and collapsing all components to points gives a p-periodic tree.

If A is irreducible and imprimitive of index p, it has a Frobenius normal form with a block structure similar to R in (3), except the non-0 blocks need not be quadratic. So the family of edges is a disjoint union of $E_1,\dots,E_p$ with $f_c: E_j\to E_{j+1}, E_p\to E_1$. There is a corresponding subdivision of the Hubbard tree into p subsets; these are disjoint except for common vertices, and we do not need to show that they are connected. Since every subset is mapped into itself under kp iterations only, every edge has return numbers divisible by p. Every characteristic periodic point has a ray period divisible by p. If c is not satellite renormalizable, the preperiodic critical value c or the primitive characteristic point z_1 is approached from below by primitive characteristic points x_n of minimal periods, which are increasing and divisible by p. Thus for large n, the internal address of x_n will be ending on $\dots$–Per(x_{n-1})–Per(x_n), so x_n is p-renormalizable according to [10]. The same applies to c, since that renormalization locus is closed. ∎

Remark 3.10 (Same entropy for different Hubbard trees)
1. For any postcritically finite parameter not on the real axis, there are corresponding parameters with a homeomorphic Hubbard tree, but different rotation numbers at periodic branch points [10]. These parameters have the same core entropy: neither the Markov matrix A nor the Thurston matrix F according to Proposition 3.5 depends on the rotation numbers. The dynamics of these parameters are conjugate by homeomorphisms, which are not orientation-preserving [10].

2. Suppose $p, q \geq 2$ and $\widehat{c}$ is a postcritically finite parameter in the $1/q$-limb. Consider the following parameters, whose p-renormalization is conjugate to $f_{\widehat{c}}(\widehat{z})$: c is satellite renormalizable in the $1/p$-limb, and c' is immediately crossed renormalizable in the $\frac{1}{pq}$-limb. Then $h(c) = h(c')$ although the dynamics are not conjugate globally. If $q \geq 3$ and $\widehat{c}$ is of β-type, the Markov matrices for the minimal Hubbard trees are identical in fact.

3. The Misiurewicz parameter $c = \gamma_M(3/14)$ has a few remarkable properties. The characteristic polynomial of F is $P(x) = x^4 - 3x - 2 = (x^2 - x - 1) \cdot (x^2 + x + 2)$ and A has $x \cdot P(x)$. This factorization is non-trivial, i.e., not involving roots of unity. Moreover, the first factor agrees for the primitive Mandelbrot set of period 3: the core entropy is $h(c_3) = h(c)$ but the dynamics are unrelated. $\mathscr{K}_c$ is discussed in [5, 18] in a different context: $f_c(z)$ on $\mathscr{K}_c$ is quasi-conformally conjugate to a piecewise-affine map $\pm sx - 1$ with $s^3 - s^2 + s + 2 = 0$.

Proposition 3.11 (Renormalization and entropy)
Suppose $c = c_p * \widehat{c}$ for a postcritically finite parameter $\widehat{c}$.

1. *If the center c_p is of pure satellite type, we have $h(c_p) = 0$ and $h(c) = \frac{1}{p} h(\widehat{c})$.*

2. *If c_p is a primitive center and $c = c_p * \widehat{c}$, then $h(c) = h(c_p) > \frac{\log 2}{p}$.*

3. *Consider a maximal-primitive small Mandelbrot set $\mathscr{M}_p = c_p * \mathscr{M}$ as defined above, and denote its tip by $c'_p = c_p * (-2)$. There is a sequence of Misiurewicz points $a_n \to c'_p$ on the vein behind c'_p, such that $h(a_n) > h(c'_p) = h(c_p)$.*

Item 2 means that $h(c)$ is constant on primitive Mandelbrot sets, see also Theorem 4.7. This fact will simplify various proofs in Section 4. Item 3 shows that the monotonicity from Proposition 3.7 is strict, when c and c' are separated by a maximal-primitive Mandelbrot set. According to [47], two postcritically finite parameters are separated by a root. Now there is a maximal-primitive root as well, unless both parameters are of pure satellite type or belong to the same primitive Mandelbrot set.

Proof of Proposition 3.11: 1. Suppose c is an immediate satellite center of the main cardioid, then the Hubbard tree is a star with an endpoint at $z = 0$, so $f_c(z)$ is injective on it. Moreover, the characteristic polynomial of A is $x^p - 1$ when $p \geq 3$. Both arguments give $h(c) = 0$. For a pure satellite center $c_p = c_k * \ldots * c_1$, apply Lemma 3.9.2 recursively to show $h(c_p) = 0$. The same relation gives $h(c_p * \widehat{c}) = \frac{1}{p} h(\widehat{c})$.

2. Suppose that c_p is not pure satellite renormalizable. There is an immediate satellite c_q of period q and a β-type Misiurewicz point b_k of preperiod k, such that c_p is behind the α-type Misiurewicz point $c_q * b_k$. By the estimate of lowest periods in decorations [28] we have $p \geq (k-1)q + (q+1) = kq + 1$. Monotonicity and the estimate from Proposition 3.8.2 give $h(c_p) \geq h(c_q * b_k) = \frac{1}{q} h(b_k) \geq \frac{1}{q} \frac{\log 2}{k} > \frac{\log 2}{p}$. More generally, if $c_p = c_s * c_q$ with c_s pure satellite type of period s and c_q of period q primitive and not pure satellite renormalizable, then $h(c_p) = \frac{1}{s} h(c_q) > \frac{1}{s} \frac{\log 2}{q} = \frac{\log 2}{p}$ again. Finally, for any

postcritically finite parameter $\widehat{c}$ we have $h(c_p * \widehat{c}) = \max\left\{h(c_p)\,,\, \frac{1}{p}h(\widehat{c})\right\} = h(c_p)$, since $\frac{1}{p}h(\widehat{c}) \le \frac{\log 2}{p} < h(c_p)$.

3. Suppose that c_p is primitive and maximal, not pure satellite renormalizable. For $c = a_n$, the critical value is behind the disconnected small Julia set. After p iterations it will be before the characteristic point, following its orbit but moving farther away with every p-cycle of iterations. After $pn \pm k$ iterations it will join a repelling cycle independent of n. Misiurewicz points with these properties are constructed to describe the domains of renormalization [28]; in the maximal case we may use α-type Misiurewicz points. Fixing any large n, set $c = a_{n+1}$ and $c' = a_n \succ c \succ c'_p$. We shall see that $h(c') > h(c)$.

The relevant preperiodic points exist in both Julia sets, as does the p-cycle of disconnected small Julia sets. The edges shall be corresponding as follows: first, the edges leading to the postcritical points behind the small Julia sets in T_c and $T_{c'}$ are identified. Second, preperiodic marked points of T_c between the small Julia sets are marked in $T_{c'}$ in addition to the postcritical points; by Lemma 3.6.3 this does not change the largest eigenvalue λ' of A'. Due to the identifications, the only difference of A and A' is related to a small edge at the first interior postcritical point: it has one preimage under A and two preimages under A'. Since A is primitive by Lemma 3.9.4, and $A' \ge A$ in each component, we have $\lambda' > \lambda$ according to Section 2.4. Finally, if c_p is maximal-primitive but not primitive maximal, the Misiurewicz points will belong to the same pure satellite Mandelbrot set $c_s * \mathscr{M}$, and the inequalities for $\widehat{a}_n$ are transferred to $a_n = c_s * \widehat{a}_n$ according to $h(a_n) = \frac{1}{s}h(\widehat{a}_n)$. ■

Item 2 and Lemma 3.9 show that a postcritically finite parameter $c \neq 0$ has the following property, if and only if it is neither pure satellite renormalizable nor immediately crossed renormalizable: the largest eigenvalue λ of A is simple, and there is no other eigenvalue of the same modulus. — Suppose c_p has the internal address 1–…–s–q–…–p, where s is of pure satellite type and q is primitive, then item 2 is strengthened by monotonicity to $h(c_p) > \frac{\log 2}{q}$. The estimate $h(c_p) \ge \frac{\log 2}{q}$ is due to Bruin–Schleicher [11]; equality can be ruled out by Lemma 3.9.4 as well, since c_q is not q-renormalizable with $\widehat{c} \neq 0$.

3.4 Biaccessibility dimension of postcritically finite maps

When c is a Misiurewicz point, the filled Julia set $\mathscr{K}_c$ is a countable union of arcs between periodic and preperiodic points, plus an uncountable union of accumulation points. The interior points of the arcs are pinching points, so they are biaccessible: there are at least two dynamic rays landing. Each of these points is iterated to the Hubbard tree in a finite number of steps. When c is a center, the arcs of the Hubbard tree and their preimages are meeting a dense family of Fatou basins each. For a pure satellite center, these basins have a countable family of common boundary points and accumulation points on an arc, so the biaccessible points in $\partial\mathscr{K}_c$ are countable. When c is a primitive center, or a satellite center within a primitive Mandelbrot set, the primitive small Julia sets do not have common boundary points, and there is an uncountable family of biaccessible accumulation points on every arc. In any case, a countable union of linear preimages shows that the Hausdorff dimension of biaccessing angles of rays is the same for the Hubbard tree T_c and for $\partial\mathscr{K}_c$. It is related to the core entropy $h(c)$ as follows:

Proposition 3.12 (Hausdorff dimension and Hausdorff measure)
1. *Suppose $f_c(z)$ is postcritically finite and consider the subset $\mathscr{K}'_c \subset \mathscr{K}_c$ of biaccessible*

points. The Hausdorff dimension of biaccessing angles is related to the core entropy by $b := \dim \gamma_c^{-1}(\mathcal{K}_c') = \dim \gamma_c^{-1}(T_c) = h(c)/\log 2$ *according to Thurston* [36, 21, 11, 60].

2. *When the biaccessibility dimension is* $0 < b \le 1$, *the Hausdorff measure of the external angles of the Hubbard tree satisfies* $0 < \mu_b(\gamma_c^{-1}(T_c)) < \infty$. *Taking all biaccessing angles of* $\mathcal{K}_c$, *we have* $\mu_b(\gamma_c^{-1}(\mathcal{K}_c')) = \infty$ *when* $0 < b < 1$.

The Thurston relation $h(c) = b \cdot \log 2$ will be proved in Section 4.2 under more general assumptions, using the fact that $\gamma_c : \gamma_c^{-1}(T_c) \subset S^1 \to T_c \cap \partial\mathcal{K}_c$ is a semi-conjugation from the angle doubling map $F(\varphi)$ to $f_c(z)$; this proof from [11, 60] has no essential simplification in the postcritically finite case. The following alternative argument is based on Hausdorff measure, and it gives a partial answer to a question in [36, Remark 1.1].

Proof: There is a finite number of intervals in S^1, such that $\gamma_c^{-1}(T_c)$ is obtained by removing these intervals and their preimages recursively [17, 31, 60]. Since $f_c(z)$ is even and $f_c : T_c \to T_c$ is surjective but not $2:1$ globally (unless $c = -2$), these intervals correspond to the components of $(-T_c) \setminus T_c$: if a component is attached at a pinching point in $\partial\mathcal{K}_c$, the interval of angles is obvious. If the cut point of a component is a superattracting periodic point, the interval is determined from the repelling periodic point on the boundary of the Fatou basin. E.g., for the primitive center c of period 4 in the $1/3$-limb, the initial intervals are $(9/14, 11/14)$ and $(12/15, 1/15)$ in cyclic order.

Removing preimages up to order n can be described in terms of an equidistant subdivision: there are x_n closed intervals W_j of length $C2^{-n}$ left, where C is related to the common denominator of the initial intervals. We shall see that x_n is bounded above and below as $x_n \asymp \lambda^n$ when $h(c) = \log\lambda > 0$, and obtain the Hausdorff dimension from λ. The basic idea is to consider preimages of the cut points in T_c, since preimages in other parts of $\mathcal{K}_c$ are removed together with another branch. After a few initial steps, the preimages are preperiodic and their number equals the number of preimages of certain edges. The decomposition of A from Lemma 3.9 shows that this number is growing by λ; although certain edges have fewer preimages in the case of pure satellite renormalization, these do not contain initial cut points. Now the remaining intervals have total length $x_n C2^{-n}$ given by the tails of geometric series (or their derivatives) in the halved eigenvalues of A. So $x_n \sim K\lambda^n$ asymptotically when λ corresponds to a primitive block of A and $x_n \asymp \lambda^n$ in general, since $\lambda > 1$ when pure satellite centers are excluded.

The equidistant covering of $\gamma_c^{-1}(T_c)$ by x_n intervals W_j of length $C2^{-n}$ gives the box dimension $b = \log\lambda/\log 2 = h(c)/\log 2$ and an upper estimate $\mu_b(\gamma_c^{-1}(T_c)) \le \limsup x_n(C2^{-n})^b < \infty$ when $b > 0$ according to the definition (2). Since $\gamma_c^{-1}(T_c)$ is closed and invariant under doubling $F(\varphi) = 2\varphi$, the Hausdorff dimension $\dim \gamma_c^{-1}(T_c) = b$ is obtained from Furstenberg [20, Proposition III.1]. We shall use similar arguments to show $\mu_b(\gamma_c^{-1}(T_c)) > 0$, following the exposition by Gao [22, Section 5.2.1]. Using an equidistant subdivision W_j' of length 2^{-n} still gives $\sum |W_j'|^b \asymp \lambda^n 2^{-bn} \asymp 1$. Assuming $\mu_b(\gamma_c^{-1}(T_c)) = 0$, there is a finite cover by closed intervals with $|U_i| = 2^{-n_i}$, aligned to the dyadic grids of different levels n_i, such that $\sum |U_i|^b < 1$. Define puzzle pieces by taking preimages under F^{n_i} restricted to U_i: by F-invariance there are nested puzzle pieces around the points of $\gamma_c^{-1}(T_c)$. The pieces of depth k contribute $(\sum |U_i|^b)^k$ to (2). For large n, each W_j' will be contained in a puzzle piece of large depth k, but our estimates do not give a contradiction yet: there may be several W_j' in the same piece. So, set $N = \max n_i$ and choose a puzzle piece of maximal level $\sum n_i$ for each W_j'. By induction, the level will be $\ge n - N$, since images under F^{n_i} still have maximal levels. Now there are at most 2^N

of the W'_j contained in one piece, the depth is $k \geq n/N - 1$, and

$$1 \asymp \sum_j |W'_j|^b \leq 2^N \sum_{k \sim n/N}^{\infty} \Big(\sum_i |U_i|^b \Big)^k \to 0 \quad \text{as} \quad n \to \infty \,. \tag{4}$$

This is a contradiction disproving the assumption $\mu_b(\gamma_c^{-1}(T_c)) = 0$. When $b < 1$, an arc in $(-T_c) \setminus T_c \neq \emptyset$ has disjoint preimages. In each step, their number is doubled and their individual measure is divided by $2^b < 2$, giving $\mu_b(\gamma_c^{-1}(\mathcal{K}'_c)) = \infty$. ∎

For the principal α-type Misiurewicz point c in the p/q-limb, the angles of an edge of T_c are obtained explicitly: on each side, we have a standard Cantor set, where an interval is divided into 2^q pieces recursively and the outer two intervals are kept. So for $b = 1/q$, the sum in (2) is independent of the levels of subdivision.

4 The biaccessibility dimension

A filled Julia set $\mathcal{K}_c$, or the Mandelbrot set $\mathcal{M}$, is locally connected if and only if every external ray lands and the landing point depends continuously on the angle (Carathéodory). Some possible scenarios are shown in Figure 3. It may happen that a pair of rays is approximated by pairs of rays landing together, without doing the same. Therefore we must distinguish between combinatorial biaccessibility and topological biaccessibility. However, every pinching point $z \in \mathcal{K}_c$, i.e., $\mathcal{K}_c \setminus \{z\}$ is disconnected, must be the landing point of at least two rays [35, p. 85]. Non-local connectivity of $\mathcal{M}$ would mean that $\mathcal{M}$ contains non-trivial fibers; these compact connected subsets are preimages of points under the projection $\pi_M : \partial\mathcal{M} \to S^1/\sim$ of [16] described in Section 4.5. As an alternative characterization, these subsets cannot be disconnected by pinching points with rational angles [47] (and they are disjoint from closed hyperbolic components). There is an analogous concept for Julia sets, but rational angles do not suffice to describe fibers of Julia sets for Siegel and Cremer parameters [48].

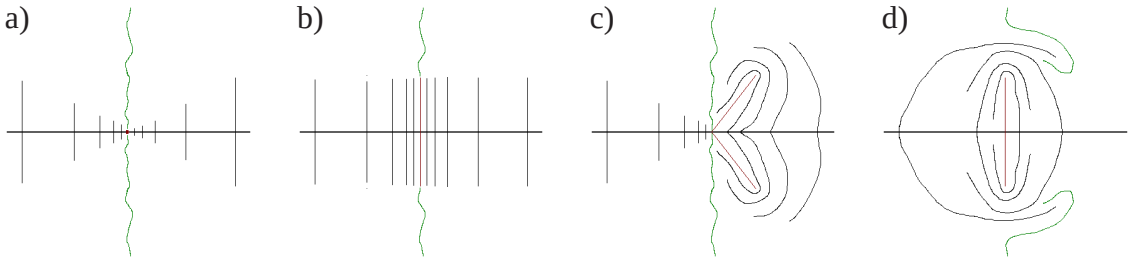

Figure 3: Possible scenarios at the Feigenbaum parameter $c_F \in \mathcal{M} \cap \mathbb{R}$: in a) $\mathcal{M}$ is openly locally connected at c_F, and the fiber of c_F is non-trivial in the other cases [16, 47]. It is formed from the impressions of two rays. In case d) the rays do not land; they have non-trivial accumulation sets. This example could be modified, such that the impressions are larger than the accumulation sets. Note that in cases b) and d), $\mathcal{M} \setminus \{c_F\}$ is not disconnected.
Similar situations arise for combinatorially biaccessing dynamic rays of a filled Julia set $\mathcal{K}_c$, but they need not be symmetric. — Non-trivial fibers may correspond to a single external ray as well.

4.1 Combinatorial and topological biaccessibility

For a given angle θ, the itinerary of φ is a sequence of symbols A, B, $*$ or 1, 0, $*$ describing the orbit of φ under doubling with respect to a partition of the circle, which is defined by the diameter joining $\theta/2$ and $(\theta+1)/2$. See [26, 49, 10]. The following result from [10, Section 9] motivates the definition of combinatorial biaccessibility by itineraries:

Lemma 4.1 (Rays landing together, Bruin–Schleicher)
Assume that $\mathcal{K}_c$ is locally connected and for some $\theta \in S^1$, $\mathcal{R}_c(\theta)$ lands at the critical value c, or θ is a characteristic angle of z_1 at the Fatou basin around c.
Suppose the rays $\mathcal{R}_c(\varphi_1)$ and $\mathcal{R}_c(\varphi_2)$ do not land at preimages of c or z_1. Then they land together, if and only if the itineraries of φ_1 and φ_2 with respect to θ are equal.

Proof: A separation line is formed by the rays $\mathcal{R}_c(\theta/2)$ and $\mathcal{R}_c((\theta+1)/2)$ together with the common landing point $z=0$; in the parabolic or hyperbolic case, there are two landing points connected with an interior arc. The itinerary of an angle with respect to θ is equal to the itinerary of the landing point with respect to the separation line, since preimages of c or z_1 are excluded. So if the landing point is the same, the itineraries coincide. Now suppose the landing points w_i of $\mathcal{R}_c(\varphi_i)$ are different: we need to show that w_1 and w_2 are separated by a preimage of $z=0$. In the case of empty interior, the arc $[w_1, w_2]$ is containing two biaccessible points w_1', w_2', which satisfy $f_c^n([w_1', w_2']) \subset [-\beta_c, \beta_c]$. The subarc covers 0 in finitely many steps, since otherwise the corresponding intervals of angles could be doubled indefinitely. If the interior of $\mathcal{K}_c$ is not empty, the arc is not defined uniquely in interior components, but an image of the subarc must cross the component around $z=0$ for the same reason. ∎

So the biaccessibility dimension will be the same for all external angles of c. If $\mathcal{K}_c$ is not locally connected, there may be pairs of rays approximated by pairs landing together, but not doing so themselves; this may look like the parameter space picture b) or d) in Figure 3, or be more complicated. With countably many exceptions, the criterion in terms of itineraries shows, which rays should land together according to the combinatorics. When θ is not periodic, for any word w angles with the itineraries $w*\nu$, $wA\nu$, and $wB\nu$ have rays landing together as well. Here ν denotes the kneading sequence, i.e., the itinerary of θ with respect to itself. If θ is periodic, you cannot see from the itinerary alone whether two angles belong to the same preimage of z_1. Again, the ambiguity concerns a countable number of angles only; it does not matter for the Hausdorff dimension:

Definition 4.2 (Biaccessibility dimension)
1. *With respect to an angle $\theta \in S^1$, φ_1 is* combinatorially biaccessing, *if there is an angle $\varphi_2 \neq \varphi_1$ such that φ_1 and φ_2 are connected by a leaf of the lamination associated to θ [56]. With countably many exceptions, this means that φ_1 and φ_2 have the same itinerary, which does not contain an $*$. The Hausdorff dimension of these angles is the* combinatorial biaccessibility dimension $B_{\text{comb}}(\theta)$.
2. *For $c \in \mathcal{M}$, an angle $\varphi_1 \in S^1$ is* topologically biaccessing, *if there is an angle $\varphi_2 \neq \varphi_1$ such that $\mathcal{R}_c(\varphi_1)$ and $\mathcal{R}_c(\varphi_2)$ land at the same pinching point $z \in \mathcal{K}_c$. The Hausdorff dimension of these angles is the* topological biaccessibility dimension $B_{\text{top}}(c)$.

The following result is basically due to Bruin and Schleicher; see the partial results in [10, Section 9] and the announcement in [11]. The proof below will discuss the dynamics of

various cases; some arguments could be replaced by the geometric observation, that the angles of non-landing rays have Hausdorff dimension 0, see the references in [11].

Theorem 4.3 (Combinatorial and topological biaccessibility)
Suppose that $\theta \in S^1$ and $c \in \partial\mathcal{M}$ belongs to the impression of $\mathcal{R}_M(\theta)$, or $c \in \mathcal{M}$ is hyperbolic and the ray lands at the corresponding root. Then $B_{\text{comb}}(\theta) = B_{\text{top}}(c)$.

Recall the notions of maximal-primitive renormalization and of pure satellite components from Section 3.3. When $f_c(z)$ is simply p-renormalizable, there is a small Julia set $\mathcal{K}_c^p \subset \mathcal{K}_c$ and $f_c^p(z)$ is conjugate to $f_{\widehat{c}}(\widehat{z})$ in a neighborhood; the hybrid-equivalence $\psi_c(z)$ is mapping $\mathcal{K}_c^p \to \mathcal{K}_{\widehat{c}}$. Now $\mathcal{K}_c \setminus \mathcal{K}_c^p$ consists of a countable family of decorations, which are attached at preimages of the small β-fixed point. Each decoration corresponds to an open interval of angles, and their recursive removal shows that the angles of rays accumulating or landing at $\partial\mathcal{K}_c^p$ form a Cantor set of Hausdorff dimension $1/p$ and finite positive Hausdorff measure [34, 28]. The parameter c belongs to a small Mandelbrot set $\mathcal{M}_p \subset \mathcal{M}$, which has corresponding decorations and the same Cantor set of angles, such that the parameter ray lands or accumulates at $\partial\mathcal{M}_p$. The Douady substitution of binary digits [15, 34] relates the external angles φ and $\widehat{\varphi}$: if $\mathcal{R}_c(\varphi)$ lands at $z \in \partial\mathcal{K}_c$, then $\psi_c(\mathcal{R}_c(\varphi))$ lands at $\widehat{z} = \psi_c(z) \in \partial\mathcal{K}_{\widehat{c}}$ and according to Liouville, $\mathcal{R}_{\widehat{c}}(\widehat{\varphi})$ lands at $\widehat{z}$ as well. The converse statement is not obvious, because $\psi_c^{-1}(\mathcal{R}_{\widehat{c}}(\widehat{\varphi}))$ may cut through the decorations. But when the "tubing" is chosen appropriately, $\mathcal{R}_{\widehat{c}}(\widehat{\varphi})$ can be deformed such that it is avoiding the images of decorations, still landing at $\widehat{z}$. The same arguments apply to parameter rays [28].

Proof of Theorem 4.3: The problem is that $\mathcal{K}_c$ may be non-locally connected; then two rays with the same kneading sequence may land at different points of a non-trivial fiber, or one may accumulate there without landing. Cf. Figure 3. By the Yoccoz Theorem [39, 25], non-local connectivity can happen only for infinitely simply renormalizable parameters c, or for $f_c(z)$ with a neutral cycle. Consider the following cases:

1. If $f_c(z)$ is hyperbolic or parabolic, $\mathcal{K}_c$ is locally connected and θ is an external angle of the characteristic point [40, 49]. If $f_c(z)$ is non-renormalizable or finitely renormalizable with all cycles repelling, $\mathcal{K}_c$ is locally connected and $\mathcal{R}_c(\theta)$ lands at the critical value: both for the dynamic plane and the parameter plane, θ is approximated by corresponding rational angles [47, 48, 49]. The statement follows from Lemma 4.1.

2. If $\mathcal{K}_c$ contains a Siegel disk or a Cremer point of period 1, we have $B_{\text{top}}(c) = 0$ [64]. If c is a Siegel or Cremer parameter on the boundary of a pure satellite component, there are countably many biaccessing angles from the satellite bifurcations. Each copy of the small Julia set has biaccessing angles of Hausdorff dimension 0, since the renormalized rays would land at $\mathcal{K}_{\widehat{c}}$. On the other hand, $B_{\text{comb}}(\theta) = 0$ according to [13, 11]. For an irrationally neutral parameter in a primitive Mandelbrot set, the biaccessibility dimension will be positive; these parameters are included in case 4.

3. Suppose the parameter c is infinitely pure satellite renormalizable. Choose a pure satellite component of period m before c and consider the angles of the rays accumulating or landing at the small Julia set and its preimages. Their Hausdorff dimension is $\frac{1}{m}$; so $B_{\text{top}}(c) \le \frac{1}{m}$ and $B_{\text{comb}}(\theta) \le \frac{1}{m}$, and letting $m \to \infty$ gives 0. All other infinitely renormalizable parameters are contained in a primitive Mandelbrot set.

4. Suppose $c = c_p * \widehat{c}$ for a primitive center c_p of period p, and denote the angles of the corresponding root by $\theta_\pm$. Since $\mathcal{R}_M(\theta)$ lands or accumulates at $\mathcal{M}_p = c_p * \mathcal{M}$, θ

belongs to the Cantor set of angles constructed above and $\mathscr{R}_c(\theta)$ accumulates or lands at $\mathscr{K}_c^p$. We will not need to check, whether it accumulates at the critical value $z = c$. By item 1, Proposition 3.11.2, and the relation to core entropy from Proposition 3.12.1, we have $B_{\text{top}}(c_p) = B_{\text{comb}}(\theta_\pm) > \frac{1}{p}$. But $\frac{1}{p}$ is the Hausdorff dimension of those angles, whose rays land or accumulate at the small Julia sets, so these are negligible. Every biaccessible point $z \in \mathscr{K}_{c_p}$ is iterated to the spine $[-\beta_{c_p}, \beta_{c_p}]$, and the angles of the spine alone have Hausdorff dimension $B_{\text{top}}(c_p)$ already. This arc consists of a Cantor set of biaccessing points (except for $\pm\beta_{c_p}$) and a countable family of interior arcs.

Each Fatou component on the spine defines a strip bounded by four dynamic rays, which are moving holomorphically for all parameters in the wake of $\mathscr{M}_p$ by the composition of Böttcher conjugations. This holomorphic motion is extended according to the Słodkowsky Theorem [50]. Neglecting branch points, the biaccessing rays of the Cantor set are approximated by strips from both sides, so their motion is determined uniquely. The moved ray is still a dynamic ray of the new polynomial, and it is still biaccessing. On the other hand, a pair of topologically biaccessing rays for the parameter $c \in \mathscr{M}_p$ is iterated to a pair separating $-\beta_c$ from β_c. Neglecting pairs separating small Julia sets, this pair belongs to the moving Cantor set. Thus $B_{\text{top}}(c) = B_{\text{top}}(c_p)$, and $B_{\text{comb}}(\theta) = B_{\text{comb}}(\theta_\pm)$ is shown analogously, observing that $\mathscr{R}_c(\theta/2)$ and $\mathscr{R}_c((\theta+1)/2)$ belong to the strip around the small Julia set at $z = 0$. ■

4.2 Core entropy revisited

According to [36, 21], the following relation is due to Thurston. The proof follows Bruin–Schleicher [11] and Tiozzo [60]. See also the partial results by Douady [17].

Theorem 4.4 (Thurston, Bruin–Schleicher, Tiozzo)
Suppose $\mathscr{K}_c$ is locally connected with empty interior, or f_c is parabolic or hyperbolic with a real multiplier. Using regulated arcs, define the tree T_c as the path-connected hull of the critical orbit. If T_c is compact, define the core entropy $h(c)$ as the topological entropy of f_c on T_c. Then it is related to the biaccessibility dimension by $h(c) = B_{\text{top}}(c) \cdot \log 2$.

Proof: First, assume that $\mathscr{K}_c$ has empty interior. According to Douady [16, p. 449], every biaccessible point $z \in \mathscr{K}_c$ has an image separating $-\beta_c$ from β_c: when two of its external angles differ in the n-th binary digit, $f_c^{n-1}(z)$ has external angles in $(0, 1/2)$ and in $(1/2, 1)$. It will be iterated to the arc of T_c through $z = 0$ in finitely many steps. Conversely, every external angle of $T_c \subset \mathscr{K}_c$ is biaccessing, with at most countably many exceptions. Setting $X_c = \gamma_c^{-1}(T_c)$ and considering a countable union of linear preimages shows $B_{\text{top}}(c) = \dim X_c$. Now X_c is forward invariant under the doubling map $F(\varphi) = 2\varphi$, which has constant slope 2. So $\log 2 \cdot \dim X_c = h_{\text{top}}(F, X_c)$ by [20, Proposition III.1]. But $\gamma_c : X_c \to T_c$ is a semi-conjugation from $F(\varphi)$ to $f_c(z)$, so $h_{\text{top}}(F, X_c) = h_{\text{top}}(f_c, T_c) = h(c)$. Note that by the Bowen Theorem [8, 37], it is sufficient that every point $z \in T_c$ has finitely many preimages under γ_c, but this number need not be bounded globally. Here every branch point with more than four branches is periodic or preperiodic by the No-wandering-triangles Theorem [56], and periodic points in $\partial\mathscr{K}_c$ are repelling. So this condition will be satisfied, even if there are infinitely many branch points.

If $f_c(z)$ is hyperbolic or parabolic, $\gamma_c(X_c) = T_c \cap \partial\mathscr{K}_c$ will be a disconnected subset of T_c. To see that $h_{\text{top}}(f_c, T_c \cap \partial\mathscr{K}_c) = h_{\text{top}}(f_c, T_c)$ in the maximal-primitive case of period

p, the estimate $h(c) > \frac{\log 2}{p}$ from Proposition 3.11.2 shows again that the interior does not contribute more to the entropy. In the pure satellite case, the number of preimages under $f_c^n(z)$ is not growing exponentially on T_c, so $h(c) = 0$. ∎

Similar techniques show that the set of biaccessing pairs $(\varphi_1, \varphi_2) \in S^1 \times S^1$ has the same Hausdorff dimension [22]. In the postcritically finite case, results on Hausdorff measure are found in Proposition 3.12. Thurston [57] has suggested to define a core $T_c \subset \mathcal{K}_c$ for every $c \in \mathcal{M}$ as "the minimal closed and connected forward-invariant subset containing [the critical point], to which the Julia set retracts." Consider the following cases:

- If c is parabolic or hyperbolic of period p, the critical orbit is connected with arcs from z to $f_c^p(z)$, but T_c will not be unique. If $\mathcal{K}_c$ contains a locally connected Siegel disk $\mathcal{D}$ of period 1, the core is $\overline{\mathcal{D}}$. For a p-cycle of locally connected Siegel disks, T_c contains arcs through preimages of these disks in addition.

- In the fixed Cremer case and in the infinitely pure satellite renormalizable case, the following situation may arise according to Douady and Sørensen [52, 53]: the rays $\mathcal{R}_c(\theta/2)$ and $\mathcal{R}_c((\theta+1)/2)$ each accumulate at a continuum containing both α_c and $-\alpha_c$. $\mathcal{K}_c$ is neither locally connected nor arcwise connected. The core according to the above definition may be too large, even all of $\mathcal{K}_c$. The same problem applies to Cremer cycles of pure satellite type, and possibly to the non-locally connected Siegel case.

- In the primitive renormalizable case, we have $h_{\text{top}}(f_c, T_c) = B_{\text{top}}(c) \cdot \log 2$ for a fairly arbitrary choice of T_c. Even if the small Julia set $\mathcal{K}_c^p$ is an indecomposable continuum, we may include complete preimages of it in T_c, because $B_{\text{top}}(c) > 1/p$.

- Suppose $\mathcal{K}_c$ is locally connected with empty interior, but the arcwise connected hull of the critical orbit is not compact. Then it is not clear, whether taking the closure of T_c may produce an entropy $h_{\text{top}}(\overline{T_c}) > B_{\text{top}}(c) \cdot \log 2$.

Remark 4.5 (Locally connected model and non-compact core)
1. For any parameter angle θ, Bruin–Schleicher [11, version 1] consider the set X_θ of angles φ that are either postcritical or combinatorially biaccessing and before a postcritical angle. In the cases where $\mathcal{K}_c$ has empty interior and is not of Cremer type, this set corresponds to a tree T_θ within a locally connected model of $\mathcal{K}_c$, which is a quotient of S^1 or of a space of itineraries. Now $h_{\text{top}}(f, T_\theta) = h_{\text{top}}(F, X_\theta) = B_{\text{comb}}(\theta) \cdot \log 2$ may be shown using a generalized notion of topological entropy when T_θ is not compact. It would be interesting to know whether the entropy on the closure can be larger, and whether T_θ can be embedded into $\mathcal{K}_c$ in the infinitely renormalizable case; probably this will not work in the situation of [53] described above.

2. Suppose the binary expansion of θ is a concatenation of all finite words. Then the orbit of θ under doubling is dense in S^1. The parameter c is not renormalizable and not in the closed main cardioid, so $\mathcal{K}_c$ is locally connected with empty interior. Since the critical orbit is dense in $\mathcal{K}_c$, the tree T_θ corresponds to a non-compact union T_c of a countable family of arcs in $\mathcal{K}_c$. Now $B_{\text{top}}(c) = \dim \gamma_c^{-1}(T_c) < 1 = h_{\text{top}}(\overline{T_c})/\log 2$ shows that the generalized topological entropy satisfies $\dim \gamma_c^{-1}(T_c) \neq h_{\text{top}}(T_c)/\log 2$ or $h_{\text{top}}(T_c) < h_{\text{top}}(\overline{T_c})$.

4.3 Monotonicity, level sets, and renormalization

Monotonicity of the biaccessibility dimension (or core entropy) has been shown by Penrose [44] for abstract kneading sequences and by Tao Li [31] for postcritically finite polynomials, cf. Proposition 3.7. In terms of angles it reads as follows:

Proposition 4.6 (Monotonicity of laminations, folklore)
Suppose $\theta_- < \theta_+$ are such that for some parameter c, the corresponding dynamic rays land together at the critical value c, or $\theta_\pm$ are characteristic angles at z_1. If an angle φ is combinatorially biaccessing with respect to $\theta_\pm$, it stays biaccessing for all angles $\theta \in (\theta_-, \theta_+)$. In particular we have $B_{\text{comb}}(\theta) \geq B_{\text{comb}}(\theta_\pm)$.

The assumption may be restated in terms of laminations of the disk [56] as follows: $\theta_\pm$ belong to a leaf or a polygonal gap of the quadratic minor lamination QML. If c is a branch point, we may assume that $\theta_\pm$ bound the whole wake. Their preimages divide the circle into four arcs; the preimages of θ are contained in $I_0 = (\theta_-/2, \theta_+/2)$ and $I_1 = ((\theta_-+1)/2, (\theta_++1)/2)$. Consider the set $B \subset S^1$ of angles combinatorially biaccessing with respect to $\theta_\pm$, and the subset $U \subset B$ of biaccessing angles φ that are never iterated to $I_0 \cup I_1$ under doubling $F(\varphi) = 2\varphi$. For each $\varphi \in U$ the itinerary with respect to θ_- is the same as the itinerary with respect to θ_+. Now B is the union of iterated preimages of U and $B_{\text{comb}}(\theta_\pm) := \dim B = \dim U$. To see this, we may assume that c belongs to a vein according to Proposition 4.8; otherwise c would have a non-trivial fiber intersecting a vein and it should be moved there. Then $\mathcal{K}_c$ is locally connected, the beginning of the critical orbit is defining a finite tree $T_c \subset \mathcal{K}_c$, and every biaccessible point is iterated to $T_c \cap \partial\mathcal{K}_c$. Moreover, T_c does not have external angles in $I_0 \cup I_1$, since no $z \in T_c \cap \partial\mathcal{K}_c$ is iterated behind c or z_1. So both U and B are iterated to $\gamma_c^{-1}(T_c \cap \partial\mathcal{K}_c)$. Variations of the following argument where used by Douady [17] in the real case, by Tao Li [31] in the postcritically finite case, and by Tan Lei for veins [60, Proposition 14.6].

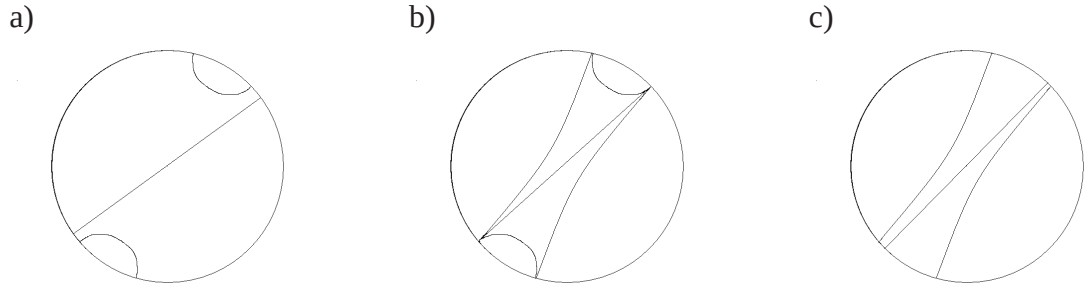

Figure 4: The pattern of rays landing together can be described by a lamination of the disk [56]. As θ is varied, the diameter defined by $\theta/2$ and $(\theta+1)/2$ is moving and disconnecting or reconnecting chords. The closed lamination is describing combinatorially biaccessing pairs of angles; the corresponding rays need not land together if $\mathcal{K}_c$ is non-locally connected.

Proof of Proposition 4.6: The itinerary of any pair $\varphi_1, \varphi_2 \in U$ remains the same for all angles $\theta \in (\theta_-, \theta_+)$, so φ_1 and φ_2 remain biaccessing. Their preimages in B remain biaccessing as well. As an alternative argument, consider the possible change of partners for $\varphi \in B$ according to Figure 4: since φ is iterated through $I_0 \cup I_1$ and (θ_-, θ_+) a finite number of times, it has a finite number of possible itineraries with respect to $\theta \in (\theta_-, \theta_+)$. Now φ is changing the partner when θ is an iterate of φ or conjugate to an iterate of φ.

The partners remain faithful on the finite number of remaining intervals for θ, since their itineraries do not change there. ∎

So, what kind of bifurcation is changing the biaccessibility dimension? The bifurcation of rational rays at a root is known explicitly, but it does not affect the dimension. The periodic pairs stay the same for parameters in the wake, while preperiodic and irrational pairs may be regrouping. Now the dimension is changed only when an uncountable family of irrational angles is gaining or losing partners. The bifurcations should be studied for real parameters first: with $\|\varphi\| := \min\{\varphi, 1-\varphi\}$, and real $c = \gamma_M(\theta)$, the external angles φ of the Hubbard tree $[c, f_c(c)]$ are characterized by $\|F^n(\varphi)\| \le \|\theta\|$ for all $n \ge 0$. All biaccessible angles satisfy $\|F^n(\varphi)\| \le \|\theta\|$ for $n \ge N_\varphi$. E.g., $\varphi = 0.010010001\ldots$ is biaccessible for $c = -2 = \gamma_M(1/2)$ but not for any other real parameter.

Suppose $c_n \nearrow c_0$ with $B_{\text{top}}(c_n)$ strictly increasing. Denote the sets of biaccessing angles by B_n and B_0. Consider the union $B_- = \bigcup B_n$ and the newly biaccessible angles $B_+ = B_0 \setminus B_-$. Then it will be hard to prove $\dim B_n \to \dim B_0$ by estimating $\dim B_+$, since we have $\dim B_- = \lim \dim B_n \le \dim B_0 = \dim B_+$ in general. The last equality is obtained by considering the Hausdorff measure for $b = \dim B_0$: now $\dim B_n < b$ gives $\mu_b(B_-) = 0$, but $\mu_b(B_0) > 0$ according to Proposition 3.12.

For pure satellite renormalization, the relation $B_{\text{top}}(c) = \frac{1}{p} B_{\text{top}}(\widehat{c})$ from Proposition 3.11.1 extends to all parameters $\widehat{c} \in \mathcal{M}$ by the Douady substitution of binary digits [15, 28], since the covering intervals of length 2^{-np} correspond to intervals of length 2^{-n}. The scaling implies that $B_{\text{top}}(c) \to 0 = B_{\text{top}}(c_0)$ for a pure satellite Feigenbaum point c_0 and $c \searrow c_0$ on the vein behind it. Consider primitive renormalization:

Theorem 4.7 (Strict monotonicity and primitive Mandelbrot sets)
1. *The topological biaccessibility dimension is $B_{\text{top}}(-2) = 1$ and $B_{\text{top}}(c) = 0$ for parameters c in the closed main cardioid, in closed pure satellite components, and for infinitely pure satellite renormalizable parameters. We have $0 < B_{\text{top}}(c) < 1$ for all other $c \in \mathcal{M}$.*

2. *For $c \prec c'$ we have $B_{\text{top}}(c) \le B_{\text{top}}(c')$. When $B_{\text{top}}(c') > 0$, the inequality is strict unless c and c' belong to the same primitive Mandelbrot set.*

3. *The biaccessibility dimension $B_{\text{top}}(c)$ is constant on every primitive Mandelbrot set $\mathcal{M}_p = c_p * \mathcal{M}$. Every connected component of a level set $\{c \in \mathcal{M} \,|\, B_{\text{top}}(c) = b > 0\}$ is either a maximal-primitive Mandelbrot set or a single point.*

4. *For the primitive $\mathcal{M}_4 \subset \mathcal{M}_{1/3}$ there is a sequence of parameters $c_n \in \mathcal{M} \setminus \mathcal{M}_4$ converging to the root of $\mathcal{M}_4$, such that $B_{\text{top}}(c_n) = B_{\text{top}}(\mathcal{M}_4)$.*
There is a sequence of parameters $c_n \in \mathcal{M} \setminus \{\mathrm{i}\}$ converging to the non-renormalizable Misiurewicz point $c = \mathrm{i}$, such that $B_{\text{top}}(c_n) = B_{\text{top}}(\mathrm{i})$.

Analogous statements hold for $B_{\text{comb}}(\theta)$. When $B_{\text{top}}(c)$ is restricted to a vein, items 1–3 imply that it is constant before a Feigenbaum point, and on any arc corresponding to a primitive small Mandelbrot set. For principal veins this was shown independently by Tiozzo [60]. See also the historical remarks after Theorem 4.9.

Proof of Theorem 4.7:
1. $B_{\text{top}}(-2) = 1$ is obtained from $\mathcal{K}_{-2} = [-2, 2]$ or from the 1×1-Markov matrix $A = (2)$. The pure satellite case was discussed in the proof of Theorem 4.3. In the remaining cases, $B_{\text{top}}(c) > 0$ follows from Proposition 3.11.2 and monotonicity, or from the estimate L_2 in [11]. See [67, 51, 10, 36, 11] for $B_{\text{top}}(c) < 1$.

2. There are angles $\theta_- \le \theta \le \theta_+$, such that $\theta_\pm$ are external angles of c and $\mathscr{R}_M(\theta)$ accumulates or lands at c', or at the corresponding root, or at a small Mandelbrot set around the fiber of c'. The monotonicity statement of Proposition 4.6 is transferred to the parameter plane. Under the additional assumptions, the parameters are separated by a maximal-primitive Mandelbrot set [47], and Proposition 3.11.3 gives strict monotonicity.

3. On a primitive Mandelbrot set, the biaccessibility dimension is constant by the proof of Theorem 4.3. The components of $\mathscr{M} \setminus \mathscr{M}_p$ are attached to $\mathscr{M}_p$ at the root and at Misiurewicz points. If $\mathscr{M}_p$ is maximal in the family of primitive Mandelbrot sets, these points are approached by smaller maximal-primitive Mandelbrot sets, so $B_{\text{top}}(c)$ is strictly larger behind the Misiurewicz points. For the same reason, it is strictly smaller on the vein before the root, but not necessarily on branches at the vein, see item 4. If $B_{\text{top}}(c) > 0$ and c is not primitive renormalizable, then it is at most finitely renormalizable with all cycles repelling, so its fiber is trivial by the Yoccoz Theorem. It can be separated from any other parameter by a maximal-primitive Mandelbrot set again.

4. Denote the root by c_* in the first case, and $c_* = \mathrm{i}$ in the second case. Define a_n as the sequence of α-type Misiurewicz points of lowest orders before c_*, then $B_{\text{top}}(a_n) < B_{\text{top}}(c_*)$ by item 2. In the other branch of a_n, the β-type Misiurewicz point of lowest order satisfies $B_{\text{top}}(b_{n\pm1}) > B_{\text{top}}(c_*)$ by Examples 6.5 and 6.3, respectively. Continuity on the vein to $b_{n\pm1}$ according to Theorem 4.9 provides a parameter c_n on the arc from a_n to $b_{n\pm1}$ with $B_{\text{top}}(c_n) = B_{\text{top}}(c_*)$. ∎

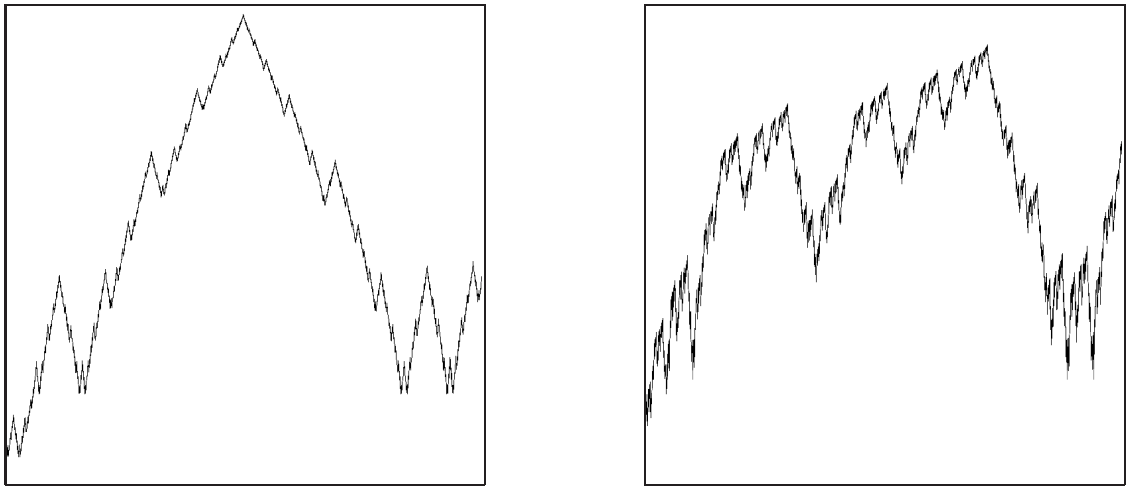

Figure 5: The graph of $\lambda(\theta)$ representing $B_{\text{comb}}(\theta)$ on intervals containing $[3/7, 25/56]$ and $[3/15, 49/240]$, which are corresponding to one decorated side of the primitive Mandelbrot sets $\mathscr{M}_3$ and $\mathscr{M}_4$. Note that in both cases, p-renormalizable angles are on the same level and most of the interval represents the $1/3$-limb. There seems to be a left-sided maximum at $3/7$ but not at $3/15$. In both cases there is a similarity between the various sublimbs; see Figure 7 for $\mathscr{M}_4$. In the case of $\mathscr{M}_3$, the symmetry of the $1/2$-limb seems to be transferred to other sublimbs.

4.4 Entropy and biaccessibility on veins

Summarizing some classical results:

Proposition 4.8 (The tree of veins, folklore)
1. *Every β-type Misiurewicz point is connected to 0 by a unique regulated arc within $\mathscr{M}$. These arcs form an infinite tree; its branch points are Misiurewicz points and centers. The tree is the disjoint union of veins, such that veins of higher preperiods branch off from a vein of lower preperiod.*

2. *Every biaccessible parameter belongs to a vein, and the corresponding dynamic rays land at the critical value or at the characteristic point. Hyperbolicity is dense on every vein.*

3. *For every parameter c on a vein, $\mathscr{K}_c$ is locally connected and the regulated path-connected hull T_c of the critical orbit is a finite tree. We have $T_c \subset \widetilde{T}_c$, where the tree $\widetilde{T}_c$ is homeomorphic to the Hubbard tree of the β-type endpoint of the vein.*

Note that it is not known, whether $\mathscr{M}$ is locally connected on a vein; this is open for Feigenbaum points in particular. The vein has a linear order $\prec$ extending the partial order of $\mathscr{M}$ to interior parameters and to possible non-accessible boundary points.

Proof: 1. The veins were described by Douady–Hubbard in terms of the partial order $\prec$ in a locally connected Model of $\mathscr{M}$ [16]. To see that they are topological arcs, note that any non-trivial fiber would be infinitely renormalizable according to Yoccoz [25]; but a vein meets a small Mandelbrot set in a quasi-conformal image of a real interval, plus finitely many internal rays in satellite components. This argument is due to Kahn [16, 48], and homeomorphisms from intervals onto complete veins are due to Branner–Douady and Riedl [9, 46]. By the Branch Theorem [47, 56], the tree branches at Misiurewicz points with finitely many branches and at centers with countably many internal rays leading to sublimbs. There is a unique branch of lowest preperiod, since any open interval contains a unique dyadic angle of smallest denominator. By this order, the decomposition into veins is well-defined: the branch of lowest order is continued before the branch point.

2. If c is a biaccessible parameter, it is on the vein to the β-type Misiurewicz point of lowest preperiod in its wake, which corresponds to the dyadic angle of lowest preperiod in an interval. Hyperbolicity is dense on the real axis according to Graczyk–Swiątek and Lyubich [23, 33], so possible non-trivial fibers can meet it in a single point only, as illustrated in Figure 3. Triviality of fibers is preserved under tuning [48], so all non-hyperbolic parameters on a vein are roots or separated by roots, and approximated by hyperbolic arcs. The approximation by roots shows in addition, that c or z_1 has the same characteristic angles as the parameter, employing the approximation by corresponding characteristic points and local connectivity of $\mathscr{K}_c$ from item 3. — Suppose that $c \in \mathscr{M}$ and the critical value $c \in \mathscr{K}_c$ is biaccessible. It is not known whether this implies that c belongs to a vein of $\mathscr{M}$; otherwise c belongs to a non-trivial fiber crossing the candidate vein.

3. The Julia sets of real polynomials are locally connected according to Levin–van Strien [30]. If $\mathscr{K}_c$ was not locally connected, it would be infinitely simply renormalizable and obtained by tuning from a real parameter; but local connectivity would be carried over according to Schleicher [48]. Consider the tree $\widetilde{T}_c$ of regulated arcs in $\mathscr{K}_c$ connecting the orbit of a preimage of β_c corresponding to the endpoint of the vein. The beginning of the critical orbit gives the endpoints of T_c by the same arguments as for postcritically finite Hubbard trees. $\widetilde{T}_c$ is forward invariant and contains the critical value $z = c$ according to item 2, thus the entire critical orbit, so $T_c \subset \widetilde{T}_c$. The tree $\widetilde{T}_c$ bifurcates only at parameters on veins of lower order (and not at the origin of a non-principal vein). The topological

entropy on T_c and $\widetilde{T}_c$ is the same; for postcritically finite dynamics this is Lemma 3.6.4, and the general case is obtained from a recursion for the number of preimages of $z = 0$ on $\widetilde{T}_c \setminus T_c$. ■

Theorem 4.9 (Biaccessibility and entropy on veins of $\mathscr{M}$, generalizing Tiozzo)
On any vein v of $\mathscr{M}$, we have:

1. *The Hubbard tree T_c is a finite tree for $c \in v$, thus compact, and the core entropy satisfies $h_{\text{top}}(f_c, T_c) = h(c) = B_{\text{top}}(c) \cdot \log 2$.*
2. *It is 0 on an arc through pure satellite components, constant on the arcs corresponding to maximal-primitive Mandelbrot sets, and strictly increasing otherwise.*
3. *The core entropy $h(c)$ and biaccessibility dimension $B_{\text{top}}(c)$ are continuous on $\overline{v}$.*
4. *The Hausdorff dimension of biaccessing parameter angles of v before c equals $B_{\text{top}}(c)$.*

Item 1 is obtained from Proposition 4.8.3 and Theorem 4.4, and item 2 follows from Theorem 4.7. Continuity is proved below. See Proposition 5.1 for item 4. Tiozzo [60] has obtained these results for principal veins with different methods, e.g., combinatorics of dominant parameters, piecewise-linear maps on trees, and a kneading determinant. Probably continuity can be proved with the approach of Bruin–Schleicher [11] as well.

The real interval $[-2, 0]$ is the principal vein of the $1/2$-limb. Here Milnor–Thurston [38] constructed a semi-conjugacy from $f_c(z)$ to a tent map and showed that the topological entropy depends continuously and monotonically on the kneading invariant. Later the Douady map $\Phi_M(c) := \Phi_c(c)$ implied monotonicity with respect to the parameter c, by relating the symbolic description to the external angle of c [17]. An alternative proof is due to Tsujii [62, 41].

The following proofs are based on continuity results for the entropy of tree endomorphisms. Now the Hubbard tree T_c or $\widetilde{T}_c$ is homeomorphic to a linear tree and $f_c(z)$ is conjugate to a tree map, but it would be difficult to control parameter dependence of the homeomorphisms. Instead only one polynomial is transferred to a linear tree and perturbed continuously there; combinatorics relates postcritically finite maps back to polynomials. The second proof is motivated by the idea of [17] for real polynomials, but it needs deeper results on tree endomorphisms than the first one.

First proof of continuity on veins: The core entropy is constant on closed arcs corresponding to small Mandelbrot sets of maximal-primitive type. If the origin of the vein v is a pure satellite center, then $h(c)$ is 0 on a closed arc meeting pure satellite components, and it is continuous at the corresponding Feigenbaum point by tuning. Since $h(c)$ is monotonic, we need to show that it does not jump. Suppose c_0 is behind the Feigenbaum point and not primitive renormalizable. Then c_0 has trivial fiber [47] and is not a satellite root, so it is approximated monotonically from below by Misiurewicz points c_n. In the Hubbard tree $T_{c_0} \subset \mathscr{K}_{c_0}$ denote the characteristic point corresponding to c_n by z_n, then $z_n \to z_0$ from below. Now the tree T_{c_0} is homeomorphic to a tree consisting of line segments, with a map $g_0(x)$ conjugate to $f_{c_0}(z)$ and points x_n corresponding to z_n. Choose x'_n with $x_{n-1} \preceq x'_n \prec x_n$, such that the orbit of x_n does not return to $(x'_n, x_0]$, and define a sequence of continous maps $\eta_n(x)$ with $\eta_n : [x'_n, x_0] \to [x'_n, x_n]$ monotonically and $\eta_n(x) = x$ for x before x'_n, such that $g_n = g_0 \circ \eta_n \to g_0$ uniformly. Then $\liminf h_{\text{top}}(g_n) \geq h_{\text{top}}(g_0) = h(c_0)$ according to [32]. But $g_n(x)$ is postcritically finite with the same order of the critical orbit as $f_{c_n}(z)$, which implies $h_{\text{top}}(g_n) = h(c_n)$ since lap numbers of iterates are determined by itineraries on the tree. By monotonicity we have $\limsup h(c_n) \leq h(c_0)$. So there is

no jump of $h(c)$ for $c \to c_0$ from below. The construction of $g_n(x)$ needs to be modified when c_0 is a maximal-primitive root, since z_0 is strictly before the critical value c_0 : all arcs through Fatou basins are squeezed to points first. (By Proposition 3.11.2, this does not change the core entropy.)

Now suppose c_0 is behind the Feigenbaum point and either a maximal-primitive tip or not primitive renormalizable, so $h(c_0) = \log \lambda_0 > 0$. According to [2], λ_0 is the growth rate of lap numbers, $\lim \frac{1}{n} \log L(f_{c_0}^n) = h(c_0)$. For $\lambda > \lambda_0$ there is an N with $L(f_{c_0}^n) \le \lambda^n$ when $n \ge N$. Lap numbers are changing at postcritically finite parameters in v only, since the existence and the linear order of endpoints of laps is determined from their itineraries. So there is a one-sided neighborhood $U = [c_0, c') \subset v$ with $c' \succ c_0$, such that the lap number $L(f_c^n)$ is constant for $c \in U$ when $n \le N$. Since each $f_c(z)$ on T_c is conjugate to a tree endomorphism, its entropy is related to the growth of lap numbers. Now these are sub-multiplicative, so $L(f_c^{kN}) \le [L(f_c^N)]^k \le \lambda^{kN}$ and letting $k \to \infty$ gives $\log \lambda_0 = h(c_0) \le h(c) \le \log \lambda$. This shows continuity of $h(c)$ for $c \to c_0$ from above by taking $\lambda \searrow \lambda_0$. ∎

On the real vein, continuity was proved by different methods in [38, 42, 17]. The typical counterexample to continuity involves a change of the lap number $L(g^1)$ or a modification of a 0-entropy map with a periodic kink. According to [42, 2], a continuous piecewise-monotonic interval map $g_0(x)$ has the following properties under a C^0-perturbation $g(x)$ respecting the lap number: the topological entropy is lower semi-continuous for $g \to g_0$ and it can jump at most to $\frac{q}{p} \log 2$, if $g_0(x)$ has a p-cycle containing q critical points. Continuity is obtained when $h_{\text{top}}(g_0) \ge \frac{q}{p} \log 2$ already, or from C^2-convergence.

These results were generalized to non-flat piecewise monotonic-continuous maps in [43]. The highest possible jump is bounded by $\limsup h_{\text{top}}(g) \le \max(h_{\text{top}}(g_0), \log \lambda)$, where λ is the highest eigenvalue of the transition matrix describing the orbits of critical points and points of discontinuity, as long as these are mapped to each other in a finite number of iterations. By concatenating the edges, any continuous tree map can be described by a piecewise continuous interval map; if the topological entropy is discontinuous, the bound λ is related to the orbits of critical points and branch points. For quadratic polynomials, the critical point is never a periodic branch point, and a cycle of branch points gives $\lambda = 1$. By Proposition 3.11.2, a center has $h(c_p) > \frac{1}{p} \log 2$ unless it is of pure satellite type. So:

Suppose $g_0(x)$ is an endomorphism of a finite linear tree T with $h_{\text{top}}(g_0) > 0$, which is topologically conjugate to a quadratic polynomial $f_c(z)$ on T_c. Then $h_{\text{top}}(g) \to h_{\text{top}}(g_0)$ when $g \to g_0$ uniformly, where the maps g^1 have the same lap number as g_0^1 on T.

Second proof of continuity on veins: Assume that the monotonic core entropy $h(c)$ has a jump discontinuity on the vein v, omitting an interval (h_0, h_1). Again by tuning, an initial pure satellite Feigenbaum point has $h(c_F) < h_0$. Choose Misiurewicz points $c_0 \prec c_1$ on v with $0 < h(c_0) \le h_0 < h_1 \le h(c_1)$. Now $f_{c_1}(z)$ on T_{c_1} is topologically conjugate to an endomorphism $g_1(x)$ on a tree consisting of line segments. It contains the orbit of a preperiodic characteristic point corresponding to c_0, so there is a continuous family $g_t(x)$, $0 \le t \le 1$, on the linear tree with $g_0(x)$ representing the combinatorics of c_0. $g_t(x)$ shall have the same critical point as $g_1(x)$. By the adaptation of [43] above, the topological entropy of $g_t(x)$ could be discontinuous only when the critical point is p-periodic and $h_{\text{top}}(g_t) < \frac{1}{p} \log 2$; there would be a center $c \in v$ with the same order of the critical orbit [10] and $h(c) > \frac{1}{p} \log 2$. So there are $0 \le t_0 < t_1 \le 1$ with $h_{\text{top}}(g_{t_i}) = h_i$. Since the topological entropy on the tree is determined by the growth rate of lap numbers according to [2],

and lap numbers are changing only at postcritically finite parameters, there is a t with $t_0 < t < t_1$ and $h_0 < h_{\text{top}}(g_t) < h_1$, such that $g_t(x)$ is postcritically finite. Again, the critical orbit is defining an oriented Hubbard tree and there is a unique quadratic polynomial $f_c(z)$ with the same dynamics. The parameter c with $c_0 \prec c \prec c_1$ and $h_0 < h(c) < h_1$ contradicts the assumed jump discontinuity. ■

The proofs did not use the semi-conjugation from $f_c(z)$ to a piecewise-linear map of slope λ [4]. An alternative proof might be given recursively by showing that the set of admissible λ is connected for a particular shape of the tree. For principal veins, the piecewise-linear model was described explicitly in terms of external angles [60].

4.5 Continuity with respect to the angle and the parameter

Monotonicity and continuity of the core entropy on veins implies:

Proposition 4.10 (Partial results on continuity)
1. *The biaccessibility dimension $B_{\text{top}}(c)$ is continuous on the union of regulated arcs connecting a finite number of postcritically finite parameters within $\mathscr{M}$.*

2. *Suppose that $\theta_0 \in S^1$ and $c_0 \in \partial\mathscr{M}$ belongs to the impression of $\mathscr{R}_M(\theta_0)$. Assume that c_0 is biaccessible, postcritically finite, simply renormalizable, or in the closed main cardioid. Then the biaccessibility dimension is lower semi-continuous as $\theta \to \theta_0$ or as $c \to c_0$: we have $\liminf B_{\text{comb}}(\theta) \geq B_{\text{comb}}(\theta_0)$ and $\liminf B_{\text{top}}(c) \geq B_{\text{top}}(c_0)$.*

Proof: 1. Continuity on veins was shown in Section 4.4. If a postcritically finite parameter is not on a vein, it is a Misiurewicz point of period > 1 with one external angle, and $\mathscr{M}$ is openly locally connected at this point. So an arc consisting of a countable family of subsets of veins ends at this parameter. Items 2 and 3 of Proposition 4.8 remain true for this arc, and the proofs of continuity are transferred.

2. If c_0 is renormalizable and not a primitive root, there is a biaccessible $c_1 \prec c_0$ with $B_{\text{top}}(c_0) = B_{\text{top}}(c_1)$. Monotonicity gives $B_{\text{top}}(c) \geq B_{\text{top}}(c_0)$ for $c \succeq c_1$, which is a neighborhood of c_0. If c_0 is a primitive root, a postcritically finite endpoint, or a non-renormalizable biaccessible parameter with $B_{\text{top}}(c_0) > 0$, there is a sequence of parameters $a_n \nearrow c_0$ with $B_{\text{top}}(a_n) \nearrow B_{\text{top}}(c_0)$. Now $c \to c_0$ implies that $c \succ a_n$ with $n \to \infty$. ■

According to [10] the biaccessibility of an angle φ_1 can be seen by comparing its itinerary to the kneading sequence, without knowing the second angle φ_2 : every branch of $\mathscr{K}_c$ at the landing point is characterized by an eventually unique sequence of closest precritical points. This approach was used in version 1 of [11] to obtain Hölder continuity with respect to the kneading sequence ν by estimating the number of words appearing in the itineraries of biaccessing angles. However, the proof is currently under revision:

Conjecture 4.11 (Continuity on S^1, Thurston and Bruin–Schleicher)
The combinatorial biaccessibility dimension $B_{\text{comb}}(\theta)$ is continuous on S^1. Moreover, when $\theta_0 \in \mathbb{Q}$ and $B_{\text{comb}}(\theta_0) > 0$, it is Hölder continuous at θ_0 with exponent $B_{\text{comb}}(\theta_0)$.

To transfer Hölder continuity from ν to θ, consider the intervals of angles θ where the first N entries of $\nu(\theta)$ are constant: when θ_0 is rational, they do not shrink to θ_0 faster than $\sim 2^{-N}$. The Hölder exponent may become smaller for irrational θ_0. And $B_{\text{comb}}(\theta)$ is not Hölder continuous at, e.g., the root at $\theta_0 = 0$: denote by $\theta_n = 2^{-n}$ the dyadic angle

of lowest preperiod in the limb of rotation number $1/(n+1)$. According to Example 3.2, we have $B_{\text{comb}}(\theta_n) = \log\lambda_n/\log 2$ with $\lambda_n \to 1$ and $(\lambda_n)^n = 2/(\lambda_n - 1) \to \infty$.

Consider the Feigenbaum point $c_{\text{F}} = -1.401155189$ of pure satellite period doubling. It is approximated by real Misiurewicz points or centers c_k of preperiod and period $\asymp 2^k$ and $B_{\text{comb}}(\theta_k) = B_{\text{top}}(c_k) \asymp 2^{-k}$ [54], since the tuning map $\widehat{c} \mapsto (-1) * \widehat{c}$ is halving the dimension. Repeated Douady substitution gives $\log(\theta_k - \theta_{\text{F}})^{-1} \asymp 2^k$, so $B_{\text{comb}}(\theta)$ is not Hölder continuous at θ_{F} [60]. Since $c_{\text{F}} - c_k \asymp \delta_{\text{F}}^{-k}$ with $\delta_{\text{F}} = 4.669201609$, $B_{\text{top}}(c)$ is Hölder continuous on the real axis at c_{F} with exponent $\log 2/\log\delta_{\text{F}} = 0.449806966$. Note that the biaccessibility dimension on a sequence of angles or parameters gives upper and lower bounds on a particular vein due to monotonicity, but only the lower bound applies to branches of the vein as well. The bounds at the 0-entropy locus in [11] are not restricted to veins.

Theorem 4.12 (Continuity on $\mathscr{M}$)
ASSUMING CONJECTURE 4.11, THAT $B_{\text{comb}}(\theta)$ IS CONTINUOUS ON S^1:
The topological biaccessibility dimension $B_{\text{top}}(c)$ is continuous on $\mathscr{M}$.

This implication was obtained independently by Bruin–Schleicher. Two different proofs shall be discussed here: the first one considers similar cases as in the proof of Theorem 4.3. The second one will be shorter but more abstract. See version 2 of [11] for an alternative argument based on compactness of fibers [47, 48].

First proof of Theorem 4.12: According to Theorem 4.3, $B_{\text{top}}(c)$ is determined from $B_{\text{comb}}(\theta)$ when $c \in \partial\mathscr{M}$ is in the impression of $\mathscr{R}_M(\theta)$. By the proof of that Theorem, $B_{\text{top}}(c)$ is constant on the closures of interior components, since they belong to a primitive Mandelbrot set or they are pure satellite renormalizable (non-hyperbolic components belong to non-trivial fibers [16, 47], so they are infinitely renormalizable). Now $B_{\text{comb}}(\theta)$ is continuous on a compact domain by assumption, so it is uniformly continuous.

1. Suppose $c \in \partial\mathscr{M}$ is non-renormalizable or finitely renormalizable. According to Yoccoz [25], the fiber of c is trivial; there is a sequence of open neighborhoods shrinking to c, which are bounded by parts of periodic rays, equipotential lines, and arcs within hyperbolic components. More specifically:
a) If c is not on the boundary of a hyperbolic component, $\mathscr{M} \setminus \{c\}$ has finitely many branches, and c is approximated by separating roots on every branch; their external rays are connected with equipotential lines.
b) If c is a Siegel or Cremer parameter, or the root of the main cardioid, use two external rays landing at different satellite roots, an equipotential line, and an arc within the component.
c) If c is a satellite bifurcation point, apply this construction symmetrically for both components.
d) If c is a primitive root, combine b) for the component and a) for the vein before it.
The rays and equipotential lines are used to visualize a bounded open neighborhood in $\mathbb{C}$; the relatively open neighborhood in $\mathscr{M}$ is determined by pinching points and interior arcs. When $c_n \to c$, the neighborhoods can be chosen such that the angles of the rays converge to external angles of c, so $B_{\text{top}}(c_n) \to B_{\text{top}}(c)$.

2. Suppose $c \in \partial\mathscr{M}$ is infinitely pure satellite renormalizable. It is characterized by a sequence of pure satellite components, each one bifurcating from the previous one, with periods $p_k \to \infty$ and external angles $\theta_k^- \nearrow \theta_-$ and $\theta_k^+ \searrow \theta_+$. There are two cases [28]:
a) If $p_{k+1} = 2p_k$ for $k \geq K$, c belongs to the fiber of a tuned Feigenbaum point: we have

$\theta_- < \theta_+$ and a sequence of roots with external angles $\widetilde{\theta}_k^- \searrow \theta_-$ and $\widetilde{\theta}_k^+ \nearrow \theta_+$. When $c_n \to c$, there are angles θ_n with $B_{\text{top}}(c_n) = B_{\text{comb}}(\theta_n)$ and $\theta_n \in [\theta_{k_n}^-, \widetilde{\theta}_{k_n}^-]$ or $\theta_n \in [\widetilde{\theta}_{k_n}^+, \theta_{k_n}^+]$. Now $k_n \to \infty$, so $B_{\text{top}}(c_n) \to 0 = B_{\text{top}}(c)$.
b) If $p_{k+1} \geq 3p_k$ for infinitely many values of k, we have $\theta_- = \theta_+$ and $\mathcal{M}$ does not continue beyond the fiber of c. When $c_n \to c$, there are angles θ_n with $B_{\text{top}}(c_n) = B_{\text{comb}}(\theta_n)$ and $\theta_n \in [\theta_{k_n}^-, \theta_{k_n}^+]$ with $k_n \to \infty$, so $B_{\text{top}}(c_n) \to 0 = B_{\text{top}}(c)$ again.
3. Suppose $c \in \partial\mathcal{M}$ is infinitely renormalizable and belongs to a primitive Mandelbrot set $\mathcal{M}_p$. When $c_n \to c$, $c_n \in \mathcal{M} \setminus \mathcal{M}_p$, these points belong to decorations of order tending to ∞, since there are only finitely many decorations of any bounded order, and these have a positive distance to c. By the Douady substitution, or the recursive construction of decorations, the corresponding intervals of angles tend to length 0. Since $B_{\text{comb}}(\theta)$ is uniformly continuous, and constant on the angles of rays bounding the decorations, we have $B_{\text{top}}(c_n) \to B_{\text{top}}(\mathcal{M}_p)$. Note that we do not need to show that the connecting Misiurewicz points tend to c. ∎

There is a closed equivalence relation on S^1, such that $\theta_1 \sim \theta_2$ if the corresponding parameter rays land together or their impressions form the same fiber. (The latter situation would be a tuned image of the real case sketched in Figure 3, so both rays land or none does.) Now $S^1/\sim$ is a locally connected Hausdorff space, which is the boundary of the abstract Mandelbrot set [16, 47]. The natural projection $\pi_S : S^1 \to S^1/\sim$ is continuous. By collapsing non-trivial fibers, a continuous projection $\pi_M : \partial\mathcal{M} \to S^1/\sim$ is obtained. (In Figure 3, it would map any of the latter configurations to the first one.)

Second proof of Theorem 4.12: Now there is a factorization $B_{\text{comb}} = B \circ \pi_S$ with a continuous map $B : S^1/\sim \to [0,1]$, since $\theta_1 \sim \theta_2$ implies $B_{\text{comb}}(\theta_1) = B_{\text{comb}}(\theta_2)$: Siegel and Cremer parameters are not biaccessible; parameter rays with non-trivial impressions belong to infinitely renormalizable fibers, and $B_{\text{comb}}(\theta)$ is constant on the corresponding angles; and $\mathcal{M}$ is locally connected at the remaining parameters c, as is $\mathcal{K}_c$ at c. By Theorem 4.3 and assuming Conjecture 4.11 we have $B_{\text{top}} = B \circ \pi_M$ on $\partial\mathcal{M}$ as a composition of continuous maps. The interior of $\mathcal{M}$ is treated as in the first proof above. ∎

5 Biaccessibility of the Mandelbrot set

For the Mandelbrot set, topological biaccessibility is defined by parameter rays landing together. Combinatorial biaccessibility is obtained from the equivalence relation defining the abstract Mandelbrot set $S^1/\sim$ [16, 56]; a pair of angles approximated by pairs of equivalent periodic angles is equivalent as well, and the angles are combinatorially biaccessing. The rays may fail to land together as illustrated in Figure 3. By the Yoccoz Theorem [25], this can happen only for infinitely renormalizable angles, which are negligible in terms of Hausdorff dimension [34]. Zakeri [65, 66] has shown that the biaccessing angles of $\mathcal{M}$ or $\mathcal{M} \cap \mathbb{R}$ have Hausdorff dimension 1 and Lebesgue measure 0. According to Bruin–Schleicher [10, 11], the dimension is < 1 when a neighborhood of $c = -2$ or $\theta = 1/2$ is excluded.

Proposition 5.1 (Biaccessibility dimension of arcs of $\mathcal{M}$, generalizing Tiozzo)
Suppose $c' \prec c''$ do not belong to the same primitive Mandelbrot set; c'' is biaccessible or of β-type. Consider the external angles of the regulated arc $[c', c''] \subset \mathcal{M}$. Their Hausdorff dimension is related to the dynamic one by $\dim \gamma_M^{-1}[c', c''] = B_{\text{top}}(c'')$.

Proof: 1. Suppose that c'' is a non-renormalizable Misiurewicz point. To obtain $\dim \gamma_M^{-1}[c', c''] \le B_{\text{top}}(c'')$, note that $\gamma_M^{-1}[c', c''] \subset \gamma_{c''}^{-1}[\alpha_{c''}, c'']$: any biaccessible parameter $c \in [c', c'']$ is either a satellite root or approximated by roots, and there are corresponding characteristic points in $[\alpha_{c''}, c'']$; their limit is biaccessible since $\mathscr{K}_{c''}$ is locally connected.

To show $\dim \gamma_M^{-1}[c', c''] \ge B_{\text{top}}(c'')$, choose non-renormalizable Misiurewicz points c_n with $c' \preceq c_n \prec c''$ such that $c_n \nearrow c''$, and such that the preperiodic point z_c'' corresponding to c'' moves holomorphically for c in the wake of c_1. Due to non-renormalizability, the Hubbard tree for c_n is covered by iterates of the arc $[c_n, z''_{c_n}] \subset \mathscr{K}_{c_n}$, and the related maps of angles are piecewise-linear, so $\dim \gamma_{c_n}^{-1}[c_n, z''_{c_n}] = B_{\text{top}}(c_n)$. We have $\dim \gamma_M^{-1}[c', c''] \ge \dim \gamma_M^{-1}[c_n, c''] \ge B_{\text{top}}(c_n)$, since the angles of $[c_n, z''_{c_n}] \subset \mathscr{K}_{c_n}$ remain biaccessing for parameters $c \succeq c_n$ according to Proposition 4.6; assuming that the corresponding parameter rays do not land at $[c_n, c''] \subset \mathscr{M}$ gives a contradiction at least for angles that are not infinitely renormalizable. The proof is completed by $\lim B_{\text{top}}(c_n) = B_{\text{top}}(c'')$.

2. Suppose that c'' is a non-renormalizable parameter and approximate it with non-renormalizable Misiurewicz points $c' \prec c''_n \prec c''$. Then we have $[c', c'') = \bigcup [c', c''_n]$ and $\dim \gamma_M^{-1}[c', c''] = \lim \dim \gamma_M^{-1}[c', c''_n] = \lim B_{\text{top}}(c''_n) = B_{\text{top}}(c'')$ by monotonicity and continuity according to Theorem 4.9.

3. Suppose c'' is primitive renormalizable but not pure satellite renormalizable, so it belongs to a maximal primitive Mandelbrot set of period p. The argument of case 2 applies to the corresponding root c''_* as well. We have $\dim \gamma_M^{-1}[c', c''] = \dim \gamma_M^{-1}[c', c''_*] = B_{\text{top}}(c''_*) = B_{\text{top}}(c'')$ since $\dim \gamma_M^{-1}[c''_*, c''] \le \frac{1}{p} < B_{\text{top}}(c''_*)$ by Proposition 3.11.2.

4. Suppose c'' belongs to a pure satellite Mandelbrot set of maximal period p. By neglecting finitely many angles, we may assume that c' is p-renormalizable as well. The proof of cases 1–3 can be copied, noting that now the iterates of $[c_n, z''_{c_n}] \subset \mathscr{K}_{c_n}$ cover the small Hubbard tree; in the pure satellite case the biaccessibility dimension is dominated by the small Julia set according to $B_{\text{top}}(c) = \frac{1}{p} B_{\text{top}}(\widehat{c})$. On the other hand, the statement will be false when c', c'' belong to the same primitive Mandelbrot set of period p: then $\dim \gamma_M^{-1}[c', c''] \le \frac{1}{p} < B_{\text{top}}(c'')$. ∎

More generally, c'' may be an endpoint with trivial fiber, by approximating it with biaccessible parameters [48]. Tiozzo [60] has obtained Proposition 5.1 with his proof of continuity on principal veins. The following result relates the local biaccessibility dimension of $\mathscr{M}$ to the dynamic one. Common upper and lower estimates for both quantities have been determined combinatorially for $c \to -2$ in [10, 11] and at the 0-entropy locus in [11].

Theorem 5.2 (Biaccessibility dimension of pieces of $\mathscr{M}$)
ASSUMING CONJECTURE 4.11, THAT $B_{\text{comb}}(\theta)$ IS CONTINUOUS ON S^1:

1. *Define a closed piece $\mathscr{P} \subset \mathscr{M}$ by disconnecting $\mathscr{M}$ at finitely many pinching points. Then the biaccessible parameters $\mathscr{P}'$ have* $\dim \gamma_M^{-1}(\mathscr{P}') = \max\{B_{\text{top}}(c) \,|\, c \in \mathscr{P}\}$.

2. *Suppose $c \in \mathscr{M}$ is a parameter with trivial fiber, not belonging to the closure of a hyperbolic component. For any sequence of nested pieces $\mathscr{P}_n$ with $\bigcap \mathscr{P}_n = \{c\}$ we have* $\lim \dim \gamma_M^{-1}(\mathscr{P}'_n) = B_{\text{top}}(c)$.

Proof: Intersecting $\mathscr{P}$ with the tree of veins according to Proposition 4.8 gives a countable family of full veins and finitely many truncated veins; these arcs $\mathscr{A}$ contain all biac-

cessible parameters, and truncated veins within a primitive Mandelbrot set are negligible. By Proposition 5.1 we have $\dim \gamma_M^{-1}(\mathscr{P}') = \sup \dim \gamma_M^{-1}(\mathscr{A}) \le \max\{B_{\text{top}}(c) \,|\, c \in \mathscr{P}\}$. On the other hand, this maximum is attained at a parameter $c_0 \in \partial\mathscr{M} \cap \mathscr{P}$ approximated by the β-type endpoints of veins $\mathscr{A}_n \subset \mathscr{P}$, so $\dim \gamma_M^{-1}(\mathscr{P}') \ge \limsup \dim \gamma_M^{-1}(\mathscr{A}_n) = B_{\text{top}}(c_0) = \max\{B_{\text{top}}(c) \,|\, c \in \mathscr{P}\}$. Item 2 is immediate from item 1 and continuity. ∎

6 Asymptotic self-similarity and local maxima of the biaccessibility dimension

The biaccessibility dimension $B_{\text{comb}}(\theta)$ shows Hölder asymptotics at rational angles θ_0 for specific sequences $\theta_n \to \theta_0$. The same techniques give partial results towards the Tiozzo Conjecture [60]. A self-similarity of $B_{\text{comb}}(\theta)$ for $\theta \to \theta_0$ was considered by Tan Lei and Thurston [21]; the geometric sequences suggest a possible scaling factor.

6.1 Hölder asymptotics

The following example describes sequences converging to a β-type Misiurewicz point. See Figure 1 for related zooms of $B_{\text{comb}}(\theta)$.

Example 6.1 (Asymptotics at $\theta_0 = 1/4$)
$a = \gamma_M(1/4)$ is the principal β-type Misiurewicz point in the $1/3$-limb. It is approached by the sequences c_n and a_n on the vein according to Example 3.3. $B_{\text{top}}(c_n)$ or $B_{\text{top}}(a_n)$ is given by $\log \lambda_n / \log 2$, where λ_n is the largest root of the polynomial below:
Center c_n of lowest period $n \ge 4$: $x^{n-2} \cdot (x^3 - x^2 - 2) + (x+1) = 0$
α-type Misiurewicz point a_n of preperiod $n \ge 3$: $x^{n-2} \cdot (x^3 - x^2 - 2) + 2 = 0$
In the other branch at a_{n-1}, there is a β-type Misiurewicz point b_n of preperiod $n \ge 4$: $x^{n-2} \cdot (x^3 - x^2 - 2) + 2(x-1) = 0$
These polynomials are obtained in Appendix A. They imply $\lambda_n < \lambda_0$ and give geometric asymptotics $\lambda_n \sim \lambda_0 - K \cdot \lambda_0^{-n}$ with $K > 0$ in the three cases. Here $B_{\text{top}}(a) = B_{\text{comb}}(1/4)$ is determined from λ_0, which satisfies $x^3 - x^2 - 2 = 0$.

For any β-type Misiurewicz point a, $f_a(z)$ maps the arc $[-\alpha_a, \beta_a] \to [\alpha_a, \beta_a]$ and this defines sequences of preimages of 0 and α_a, respectively, approaching β_a monotonically. There are corresponding sequences of centers c_n and α-type Misiurewicz points a_n approaching a. Their critical orbit is described as follows [29]: it stays close to the orbit of the distinguished preimage of β_c until it is close to β_c, and then it moves monotonically on $[\alpha_c, \beta_c]$ until it meets 0 or α_c. The latter steps are increased with n, while the first part of the orbit is combinatorially independent of n.

Proposition 6.2 (Asymptotics at angles of Misiurewicz points)
A β-type Misiurewicz point a is approached monotonically by a sequence of centers c_n with period n on the vein before it, such that there is no lower period behind c_n. The core entropy converges geometrically: $h(c_n) \sim h(a) - K \cdot \lambda_0^{-n}$ with $K > 0$ and $h(a) = \log \lambda_0$. The same result holds for a sequence of α-type Misiurewicz points a_n of preperiod n.

Proof: For large n, choose $n' = n - n_0$ edges on $[\alpha_c, \beta_c]$ mapped monotonically, such that they are covered by the image of a unique edge. Label them such that the former edges

are $1\dots n'$ and the latter edge is the last one. The Markov matrix A_n has the characteristic matrix $A_n - xI$ in (5), where the off-diagonal blocks are 0 except for the last column each. The top left block has dimension n' and the lower right block is independent of n, as is the last column of the lower left block. (These blocks are different for c_n and a_n.)

$$A_n - xI = \left(\begin{array}{ccccc|c} -x & & & & & 1 \\ 1 & \ddots & & & & \vdots \\ & \ddots & \ddots & & & \vdots \\ & & \ddots & \ddots & & \vdots \\ & & & 1 & -x & 1 \\ \hline & & & & * & \\ & & & & \vdots & B - xI \\ & & & & * & \end{array}\right) \tag{5}$$

The characteristic polynomial is obtained by Laplace expansion of the determinant with upper $n' \times n'$ minors and complementary lower minors. There are only two non-zero contributions; taking the first n' columns for the upper minor gives $(-x)^{n'}$ and taking the first $n'-1$ columns plus the last one gives $\pm(1+x+\ldots+x^{n'-1})$, so

$$\pm \det(A_n - xI) = x^{n'} \cdot \widetilde{P}(x) + \frac{x^{n'}-1}{x-1}\widetilde{Q}(x)\ , \tag{6}$$

taking care of the relative signs. This polynomial is multiplied with $x^{n_0}(x-1)$ and regrouped, and the largest common factor is determined. So we have $h(c_n) = \log \lambda_n$ or $h(a_n) = \log \lambda_n$, respectively, where λ_n is the largest root of an equation

$$R(x) \cdot \Big(x^n \cdot P(x) - Q(x) \Big) = 0\ . \tag{7}$$

Here $P(x)$ is monic and $P(x)$ and $Q(x)$ do not have common roots. By monotonicity and continuity on the vein according to Theorem 4.9 we have $\lambda_n \nearrow \lambda_0$, so the roots of $R(x)$ have modulus $< \lambda_0$ and they are negligible at least for large n. Then $\lambda_n^n \to \infty$ gives $P(\lambda_0) = 0 \neq Q(\lambda_0)$. Now λ_0 is a simple root of $P(x)$ and the largest in modulus; otherwise for large n, (7) would have a root larger than λ_0 or a small circle of such roots around λ_0. Rewriting this equation for λ_n and performing a fixed point iteration according to the Banach Contraction Mapping Principle gives

$$x = \lambda_0 + Q(x)\frac{x-\lambda_0}{P(x)}x^{-n} \qquad \text{and} \qquad \lambda_n = \lambda_0 + \frac{Q(\lambda_0)}{P'(\lambda_0)} \cdot \lambda_0^{-n} + \mathscr{O}(n\lambda_0^{-2n})\ . \tag{8}$$

The logarithm provides a corresponding asymptotic formula for $\log \lambda_n$. ∎

The following example shows that the phenomenon is not limited to β-type Misiurewicz points, see Figure 6. The higher period of a means that the period of c_n and the preperiod of a_n grows in steps of 2:

Example 6.3 (Asymptotics at $\theta_0 = 1/6$)
$a = \mathrm{i} = \gamma_M(1/4)$ is a Misiurewicz point of preperiod 1 and period 2 in the $1/3$-limb of $\mathscr{M}$. It is approached by the sequences c_n and a_n of lowest periods or preperiods on the arc before a. λ_n is the largest root of the following polynomial:

Center c_n of lowest period $n = 5, 7, 9, \ldots$: $x^{n-1} \cdot (x^3 - x - 2) + (x^2 + 1) = 0$
α-type Misiurewicz point a_n of preperiod $n = 3, 5, 7, \ldots$: $x^{n-1} \cdot (x^3 - x - 2) + 2 = 0$
In the other branch at a_{n+1}, consider the β-type Misiurewicz point b_n with the preperiod $n = 2, 4, 6, \ldots$: $x^{n-1} \cdot (x^3 - x - 2) - 2 = 0$
These polynomials give geometric asymptotics $\lambda_n \sim \lambda_0 \pm K \cdot \lambda_0^{-n}$ with $\lambda_n < \lambda_0$ in the first two cases. Here $B_{\text{top}}(\text{i}) = B_{\text{comb}}(1/6)$ is determined from λ_0, which satisfies $x^3 - x - 2 = 0$. The polynomial for b_n is obtained in Appendix A. It shows $\lambda_n > \lambda_0$, so $B_{\text{comb}}(\theta)$ does not have a local maximum at $\theta_0 = 1/6$ and $B_{\text{top}}(c)$ does not have a local maximum at $c = \text{i}$. See Theorem 4.7.4 for another application of b_n.

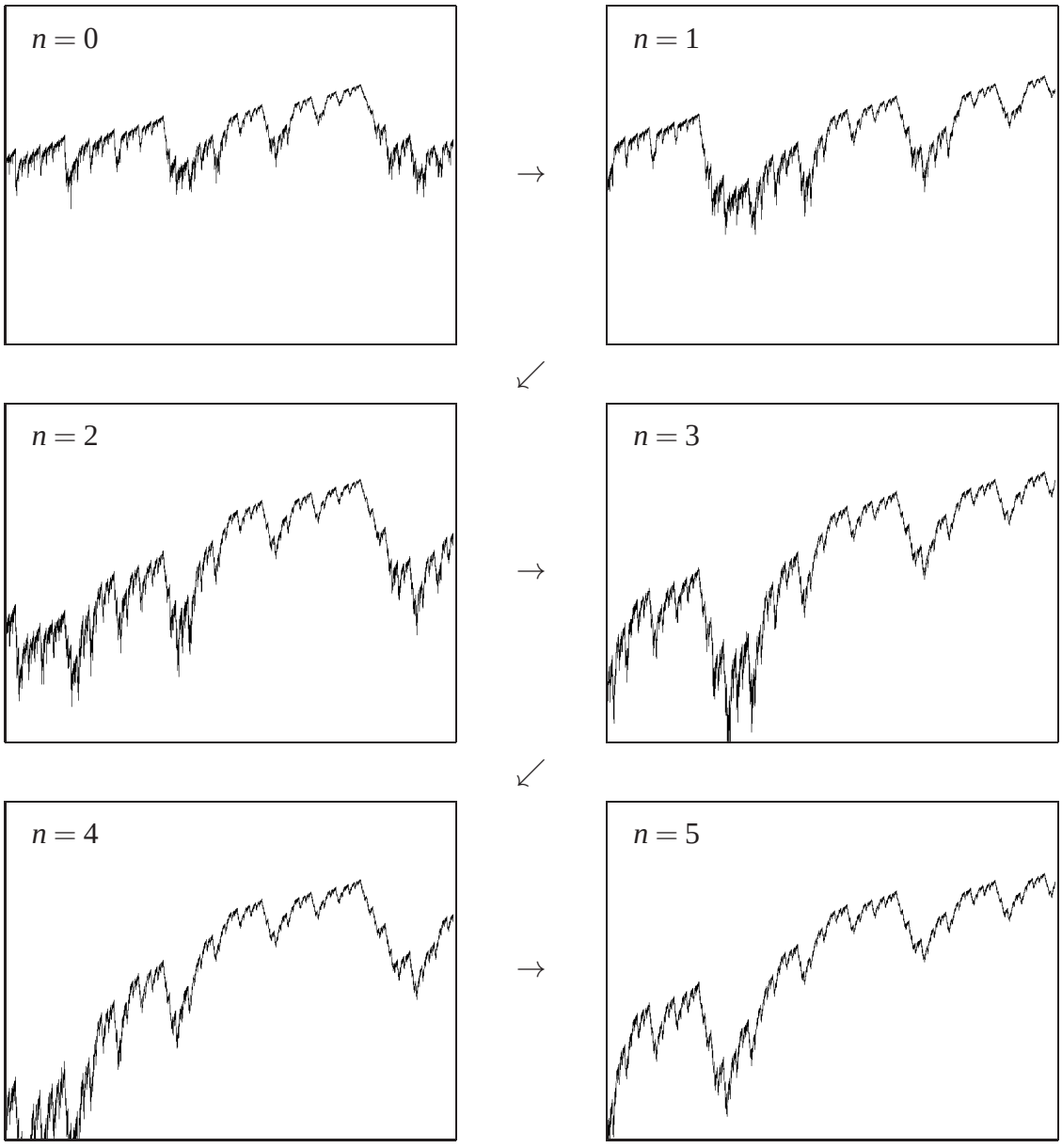

Figure 6: Consider zooms of $\lambda(\theta)$ centered at $\theta_0 = 1/6$ with $\lambda_0 = 1.521379707$. The width is 0.284×2^{-n} and the height is $2.185 \times \lambda_0^{-n}$. A left-sided maximum at θ_0 was observed by Tan Lei and Thurston [21]. There seems to be a kind of self-similarity with respect to the combined scaling by 2^2 and by λ_0^2, not by 2^1 and λ_0^1. See Example 6.3 for the asymptotics of specific sequences; one of these shows that there is not a right-sided maximum at $\theta_0 = 1/6$.

Remark 6.4 (Hölder asymptotics)
1. On every branch at a Misiurewicz point a with ray period rp, there is a sequence of centers $c_n \to a$, such that the period n is increasing by rp and there is no lower period between c_n and a. For a suitable choice of angles we have $\theta_n \sim \theta_0 \pm \widetilde{K} \cdot 2^{-n}$. In the examples given here and in Section 3.1, and for all β-type Misiurewicz points according to Proposition 6.2, we have $B_{\text{top}}(c_n) = B_{\text{comb}}(\theta_n) \sim B_{\text{comb}}(\theta_0) \pm K' \cdot \lambda_0^{-n}$ with $B_{\text{top}}(a) = B_{\text{comb}}(\theta_0) = \log\lambda_0/\log 2$. This confirms the Hölder exponent $B_{\text{comb}}(\theta_0)$ for $B_{\text{comb}}(\theta)$ at $\theta = \theta_0$ given by Bruin–Schleicher [11], see Conjecture 4.11. Similar statements apply to Misiurewicz points $a_n \to a$ and to periodic angles θ_0 with $B_{\text{comb}}(\theta_0) > 0$, see below.

2. Suppose the center parameters c_n are on an arc before or behind the Misiurewicz point a. They converge geometrically as well, $c_n \sim a + \widehat{K} \cdot \rho_a^{-rj}$ with $n = n_0 + rpj$ and the multiplier $\rho_a = (f_a^p)'(z_a)$ at the periodic point z_a [14]. By the corresponding estimate for fundamental domains [55, 29], $h(c)$ is Hölder continuous on the arc at a with the optimal exponent $h(a) \cdot p/\log|\rho_a|$. (If this was > 1, then h would be differentiable with $h'(a) = 0$.)

Example 6.5 (Asymptotics at $\theta_0 = 3/15$)
The primitive Mandelbrot set $\mathcal{M}_4$ in the $1/3$-limb of $\mathcal{M}$ has the external angles $\theta_0 = 3/15$ and $4/15$ at its root a. It is approached from below by sequences c_n and a_n of lowest period or preperiod, such that the growth factor λ_n is the largest root of the following polynomial:
Center c_n of period $n = 7, 11, 15, \ldots$: $x^n \cdot (x^4 - 2x - 1) + (x^4 + 1) = 0$
α-type Misiurewicz point a_n of preperiod $n = 3, 7, 11, \ldots$: $x^n \cdot (x^4 - 2x - 1) + 2 = 0$
In the other branch at a_{n-1}, consider the β-type Misiurewicz point b_n with the preperiod $n = 4, 8, 12, \ldots$: $x^n \cdot (x^4 - 2x - 1) - 2(x^3 + x^2 + 1) = 0$
These polynomials give geometric asymptotics $\lambda_n \sim \lambda_0 \pm K \cdot \lambda_0^{-n}$ with $\lambda_n < \lambda_0$ in the first two cases. Here λ_0 satisfies $x^4 - 2x - 1 = 0$ and $B_{\text{top}}(\mathcal{M}_4) = B_{\text{comb}}(3/15) = \log\lambda_0/\log 2$. The polynomial for b_n is obtained in Appendix A. It shows $\lambda_n > \lambda_0$, so $B_{\text{comb}}(\theta)$ does not have a left-sided local maximum at $\theta_0 = 3/15$. See Theorem 4.7.4 for another application of b_n. In the p/q-sublimb of $\mathcal{M}_4$, the β-type Misiurewicz point b'_n of lowest preperiod $n = 4q - 6 = 2, 6, 10, \ldots$ has a λ_n according to $x^n \cdot (x-1)(x^4 - 2x - 1) - 2(x^2 + 1) = 0$.

The sequence of b'_n is generalized to all hyperbolic components as follows:

Proposition 6.6 (Comparing sublimbs)
1. *Consider a hyperbolic component Ω of period m and the β-type Misiurewicz point $b_{p/q}$ of lowest preperiod $qm - m_0$ in the sublimb with rotation number p/q. Then the core entropy $h(b_{p/q}) = \log\lambda_q$ is strictly decreasing with q (and independent of p).*
2. *If Ω is not of pure satellite type, so $h(\Omega) = \log\lambda_0 > 0$, the core entropy converges geometrically: $h(b_{p/q}) \sim h(\Omega) + K \cdot \lambda_0^{-mq}$ with $K > 0$.*

Proof: We may assume $m > 1$, since the limbs of the main cardioid are treated explicitly according to Example 3.2. There is an m-cycle of small Julia sets with q branches at the small α-fixed points. For $q > 2$, label the edges such that the first one connects the critical value to a small α-fixed point, ..., edge number $q' = mq - q_0 = 1 + m(q-2)$ is an image at the same small α, and the last edge contains the critical point. When analogous edges are used for $q = 2$ as well, the cycle of small α points is marked in addition, but this does not change the highest eigenvalue of the Markov matrix A_q: the n-th order preimages of any point in the Hubbard tree are growing as λ_q^n, as does the sum of any row of A_q^n for any

subdivision into edges. The characteristic matrix $A_q - xI$ is shown in (9), where the off-diagonal blocks are 0 except for the last column each. The top left block has dimension q' and the lower right block is independent of q, as is the last column of the lower left block.

$$A_q - xI = \left(\begin{array}{ccccccc|c} -x & & & & & & & 2 \\ 1 & \ddots & & & & & & 0 \\ & \ddots & \ddots & & & & & \vdots \\ & & \ddots & \ddots & & & & \vdots \\ & & & 1 & -x & & & 0 \\ \hline & & & & & 1 & & \\ & & & & & 0 & & B - xI \\ & & & & & \vdots & & \end{array}\right) \tag{9}$$

The characteristic polynomial is obtained from Laplace cofactor expansion along the first row and multiplied with x^{q_0} afterwards. We have $h(b_{p/q}) = \log \lambda_q$, where λ_q is the largest root of an equation

$$x^{mq} \cdot P(x) - Q(x) = 0 \tag{10}$$

with $P(x)$ monic. Now $P(x) = x^k \cdot (x-1) \cdot P_0(x)$, where $P_0(x)$ is the characteristic polynomial for the center c of Ω: when the entry 2 in the first row of A_2 is omitted, this removes $Q(x)$ from the characteristic polynomial. On the other hand, the same Markov matrix will be obtained for c, when edges to preimages of β_c are added to the Hubbard tree according to Lemma 3.6.4. So $P(\lambda_0) = 0$ and $P(x) > 0$ for $x > \lambda_0$. If $\lambda_0 > 1$ then λ_0 is a simple root of $P(x)$ by Lemma 3.9.1 and Proposition 3.11.2. Now $\lambda_q > \lambda_0$ shows $P(\lambda_q) > 0$ and $Q(\lambda_q) > 0$. Setting $x = \lambda_{q+1}$ in the equation (10) for λ_q gives

$$\lambda_{q+1}^{mq} \cdot P(\lambda_{q+1}) - Q(\lambda_{q+1}) = \left(\lambda_{q+1}^{mq} - \lambda_{q+1}^{m(q+1)}\right) \cdot P(\lambda_{q+1}) < 0\,, \tag{11}$$

which implies monotonicity $\lambda_{q+1} < \lambda_q$. Set $\lambda_* := \lim \lambda_q \geq \lambda_0$. Assuming $\lambda_0 > 1$, we have $\lambda_* > 1$ and taking $x = \lambda_q$, $q \to \infty$ in (10) gives $Q(\lambda_*)/P(\lambda_*) = \infty$, so $P(\lambda_*) = 0$, $\lambda_* = \lambda_0$, and $Q(\lambda_0) \neq 0$. Geometric asymptotics are obtained as in Proposition 6.2 since $P'(\lambda_0) > 0$. The asymptotics will be different when $\lambda_0 = 1$ but we still have $\lambda_q \searrow \lambda_0$: assuming $\lambda_* > \lambda_0$ and taking $q \to \infty$ in (10) again gives the contradiction $P(\lambda_*) = 0$. ■

6.2 Local maxima

The wake of a pinching point c is bounded by two parameter rays, such that it contains all parameters $c' \succ c$. If c is a root or a Misiurewicz point, these parameter rays have rational angles. When c is a branch point, the wake consists of subwakes corresponding to the branches behind c. In the wake of a hyperbolic component, the wakes of satellite components may be called subwakes of the original component, since they correspond to sublimbs. Motivated by an analogous result for α-continued fractions, Tiozzo has conjectured that on any wake or subwake, or union of neighboring subwakes, the maximal entropy is attained at the β-type Misiurewicz point of lowest preperiod [60]. According to Proposition 4.8.1, these points are organized in an infinite tree of veins, whose branch points are centers and Misiurewicz points. This suggests to address the Tiozzo Conjecture by considering the two cases separately. The first case is Proposition 6.6.1, but the second case is still open:

Conjecture 6.7 (Comparing branches)
Consider a branch point a and for each branch behind a, the β-type Misiurewicz point of lowest preperiod. Of these, the point with the lowest preperiod has strictly maximal entropy and biaccessibility dimension.

This conjecture is equivalent to the Tiozzo Conjecture (except for neighboring subwakes of a branch point). Figure 1 suggests a local maximum of $B_{\text{comb}}(\theta)$ at $\theta_0 = 1/4$, which implies a local maximum of $B_{\text{top}}(c)$ at $c_0 = \gamma_M(\theta_0)$. On the other hand, Figure 6 implies only a left-sided maximum [21] at the external angle $\theta_0 = 1/6$ of $c_0 = \text{i}$. In Example 6.3 a sequence of β-type Misiurewicz points b_n with angles $\searrow 1/6$ and $h(b_n) > h(\text{i})$ is constructed, proving that there is no right-sided maximum at $1/6$. By Theorem 4.7.2 or Proposition 3.11.3, $B_{\text{comb}}(\theta)$ cannot be constant on an interval, since β-type Misiurewicz points are dense in $\partial\mathcal{M}$ and approximated by maximal-primitive Mandelbrot sets.

Theorem 6.8 (Maximal entropy)
1. *$B_{\text{top}}(c)$ has a local minimum at $c_0 \in \mathcal{M}$, if and only if $B_{\text{top}}(c_0) = 0$ or c_0 is primitive renormalizable and not a maximal-primitive root.*
If there is a local maximum at $c_0 \in \partial\mathcal{M}$, then c_0 is an endpoint and neither simply renormalizable nor on the boundary of the main cardioid.
Analogous statements hold for local minima and maxima of $B_{\text{comb}}(\theta)$, but there are strict local minima at the inner angles of branch points in addition,

2. *Conjecture 6.7 implies: on the interval of any wake or subwake, $B_{\text{comb}}(\theta)$ restricted to dyadic angles has a strict absolute maximum at the dyadic angle of lowest preperiod. The restriction of $B_{\text{comb}}(\theta)$ to dyadic angles will be continuous.*

3. ASSUMING CONJECTURE 4.11, THAT $B_{\text{comb}}(\theta)$ IS CONTINUOUS ON S^1:
Conjecture 6.7 implies: on any wake or subwake, $B_{\text{top}}(c)$ has a strict absolute maximum at the β-type Misiurewicz point c_0 of lowest preperiod. There will be a local maximum at $c \in \partial\mathcal{M}$, if and only if c is of β-type.

Proof: 1. Suppose $B_{\text{top}}(c_0) > 0$. If c_0 is primitive renormalizable and not a maximal-primitive root, then $B_{\text{top}}(c) \geq B_{\text{top}}(c_0)$ for c behind the corresponding primitive-maximal root c_1. Otherwise c_0 is only finitely renormalizable, so its fiber is trivial, and for c on the regulated arc before c_0 we have $B_{\text{top}}(c) < B_{\text{top}}(c_0)$ by Theorem 4.7.2.
If c_0 is simply renormalizable or on the boundary of the main cardioid, it is approximated by β-type Misiurewicz points c with $B_{\text{top}}(c) > B_{\text{top}}(c_0)$. Otherwise it has trivial fiber, so there is a finite number of rays landing, and this number must be one when there is a maximum at c_0: otherwise $B_{\text{top}}(c) > B_{\text{top}}(c_0)$ for $c \succ c_0$.

2. Fix an interval of angles corresponding to a wake and denote the dyadic angle of smallest denominator by θ_0. Choose another dyadic angle θ in the interval. Intersecting the regulated arc from $c_0 = \gamma_M(\theta_0)$ to $c = \gamma_M(\theta)$ with the tree of veins according to Proposition 4.8 gives a finite number of branch points on a finite number of veins. The first vein is ending at c_0 and the last vein at c. For each vein, the endpoint has lowest preperiod in the subwake of the origin of the vein. The finite collection of endpoints is compared successively by applying Proposition 6.6 or Conjecture 6.7 to the corresponding branch point of the tree.
A sequence of dyadic angles $\theta_n \to \theta_0$ has higher preperiods eventually. There are parameters $a_n \nearrow c_0 = \gamma_M(\theta_0)$ with $c_n = \gamma_M(\theta_n)$ behind a_n, so $B_{\text{top}}(a_n) < B_{\text{top}}(c_n) < B_{\text{top}}(c_0)$. Continuity on the vein according to Theorem 4.9 gives $B_{\text{top}}(a_n) \to B_{\text{top}}(c_0)$, which implies

$B_{\text{top}}(c_n) \to B_{\text{top}}(c_0)$ and $B_{\text{comb}}(\theta_n) \to B_{\text{comb}}(\theta_0)$.

3. Choose a non-simply-renormalizable parameter $c \in \partial\mathcal{M}$ within the given wake or subwake. c has trivial fiber. If it is not of β-type, the regulated arc from c_0 to c is meeting a countable family of veins with endpoints $c_n \to c$. The recursive application of item 2 shows that $B_{\text{top}}(c_n)$ is strictly decreasing; we have $B_{\text{top}}(c_n) \to B_{\text{top}}(c)$ by assuming continuity of $B_{\text{comb}}(\theta)$ and Theorem 4.12. So $B_{\text{top}}(c) < B_{\text{top}}(c_0)$, there is no local maximum at c, and there is a strict absolute maximum at c_0 for the given wake or subwake. ■

6.3 Self-similarity

Figures 1 and 6 suggest that the graph of the biaccessibility dimension $B_{\text{comb}}(\theta)$ may be self-similar; see also Tan Lei–Thurston [21]. According to the examples and propositions in Section 6.1, there are periodic and preperiodic angles θ_0 with the following property: $B_{\text{comb}}(\theta_0) = \log\lambda_0/\log 2 > 0$ and there is a sequence of rational angles $\theta_n \to \theta_0$ with n growing by rp, $\theta_n \sim \theta_0 + \widetilde{K}\cdot 2^{-n}$, and $B_{\text{comb}}(\theta_n) \sim B_{\text{comb}}(\theta_0) + K'\cdot\lambda_0^{-n}$. So we shall zoom into the graph by scaling with 2^{rpj} in the horizontal and by λ_0^{rpj} in the vertical direction:

- Is there a limit set for $j \to \infty$ in local Hausdorff topology [55]?
- Is it the graph of a function $S(x) = \lim \lambda_0^{rpj} \cdot \Big(B_{\text{comb}}(\theta_0 + 2^{-rpj}x) - B_{\text{comb}}(\theta_0)\Big)$, which would be self-similar under combined scaling by 2^{rp} and λ_0^{rp}?

The latter property can hold only when $\theta_n' - \theta_n = o(2^{-n})$ implies $B_{\text{comb}}(\theta_n') - B_{\text{comb}}(\theta_n) = o(\lambda_0^{-n})$, which would follow from a suitable uniform Hölder estimate for $B_{\text{comb}}(\theta)$ in a neighborhood of θ_0 [11].

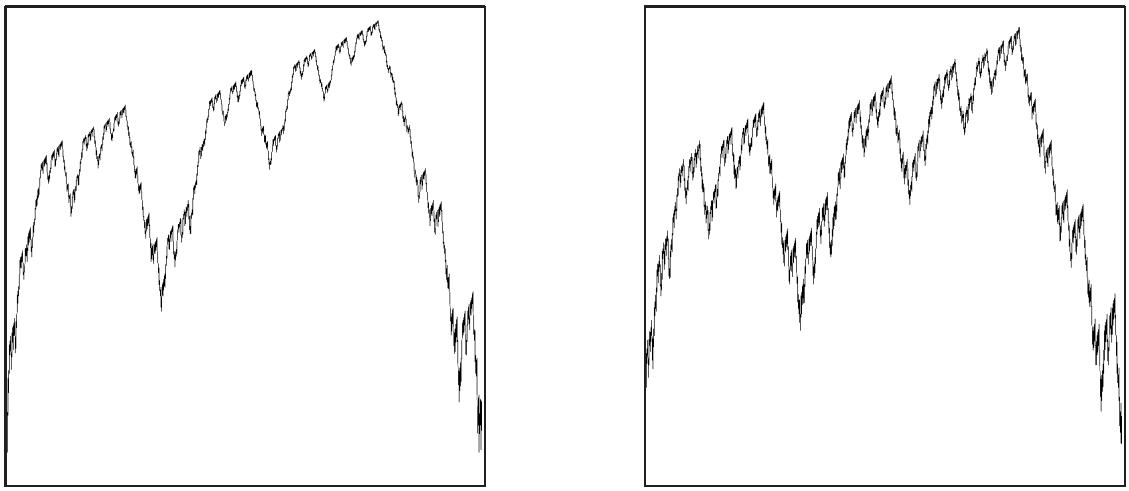

Figure 7: The graph of $\lambda(\theta)$ representing $B_{\text{comb}}(\theta)$ on the intervals $[52/255, 67/255]$ and $[820/4095, 835/4095]$, which are corresponding to the limbs $1/2$ and $1/3$ of the primitive Mandelbrot set $\mathcal{M}_4$, see also Figure 5.

A different similarity phenomenon is suggested by Figure 7. It has a qualitative explanation by the linear map between angles of α-type and β-type Misiurewicz points in different sublimbs. But this correspondence cannot describe the graph of $B_{\text{comb}}(\theta)$ in detail, because the angles of a branch point in one limb may correspond to endpoints or to several branch points in the other limb.

A Markov matrices and characteristic polynomials

Let us start with the **proof of Lemma 3.6:**
1. When c is preperiodic and the two edges at $z = 0$ are numbered first and second, the Markov matrix $\widetilde{A}$ has the block form given in (12). Note that the first two rows are identical, because no marked point is mapped to 0, so the image of any edge either covers both edges at 0 or neither. $u = 1$ or $u = 0$ indicates whether the edge intersecting $(0, \beta_c]$ is mapped over itself.

$$\widetilde{A} = \left(\begin{array}{c|c|c} 0 & u & C \\ \hline 0 & u & C \\ \hline B_1 & B_2 & D \end{array}\right) \quad \to \quad \left(\begin{array}{c|c|c} 0 & 0 & 0 \\ \hline 0 & u & C \\ \hline B_1 & B_3 & D \end{array}\right) \quad = \quad \left(\begin{array}{c|c} 0 & 0 \\ \hline B & A \end{array}\right) \tag{12}$$

A conjugate matrix is obtained by adding the first column to the second column and subtracting the second row from the first, denoting $B_1 + B_2 = B_3$. In the new block form, the second row and column may be interpreted as the transitions to and from the joint edge containing $z = 0$, so a block equal to A is identified; now $\widetilde{A}$ has the same eigenvalues as A and an additional eigenvalue 0. Note that B_3 and A have a unique entry of 2. While $\widetilde{A}$ corresponds to the usual definition of the Hubbard tree, A is used for the examples in the present paper; $\widetilde{A}$ should be used as the adjacency matrix for a subshift of finite type. — Now A is irreducible if and only if $\widetilde{A}$ is irreducible, since total connectivity of the Markov graph is transferred. Consider eigenvalues of modulus λ to show that primitivity is preserved as well.
2. The fixed point α_c is not marked when the parameter c in the $1/2$-limb is not an α-type Misiurewicz point. Splitting the edge containing α_c gives the following transition matrix $\widetilde{A}$, since the new edges at α_c are mapped over each other. The proof proceeds as in item 1 with the additional eigenvalue -1.

$$\widetilde{A} = \left(\begin{array}{c|c|c} 0 & 1 & C \\ \hline 1 & 0 & C \\ \hline B_1 & B_2 & D \end{array}\right) \quad \to \quad \left(\begin{array}{c|c|c} -1 & 0 & 0 \\ \hline 1 & 1 & C \\ \hline B_1 & B_3 & D \end{array}\right) \quad = \quad \left(\begin{array}{c|c} -1 & 0 \\ \hline B & A \end{array}\right) \tag{13}$$

3. When an edge is split by marking a preimage of a marked point, $\widetilde{A}$ will have an additional eigenvalue 0 by the same proof as for item 1.
4. When, e.g., edges towards β_c and to a first and second preimage are attached to the Hubbard tree, the new matrix has the following block form. $\widetilde{A}$ is reducible, since the original edges are not mapped to the new ones. The additional eigenvalues are 1 and 0.

$$\widetilde{A} = \left(\begin{array}{ccc|c} 0 & 0 & 0 & \\ 1 & 0 & 0 & 0 \\ 0 & 1 & 1 & \\ \hline & & & \\ & B & & A \\ & & & \end{array}\right) \tag{14}$$

■

To obtain the characteristic polynomials for a sequence of matrices, the characteristic matrix $A - xI$ may be transformed to a companion matrix with x-dependent coefficients.

When every orbit of edges is passing through a small subfamily, the rome method can be used [2]. We shall employ matching conditions for a piecewise-linear model with expansion rate $\lambda > 1$ again; as the characteristic polynomial, the resulting equation has the growth factor as its largest positive solution, since all edges have expressions for the length that are positive for $\lambda > 1$, and the topological entropy is determined uniquely by the combinatorics. Using the normalization of length 1 for $[0, \pm\alpha_c]$ for parameters c behind $\gamma_M(9/56)$, we have $2/\lambda$ for $[\alpha_c\,, \gamma_c(9/28)]$, $2/\lambda^2$ for $[\alpha_c\,, \gamma_c(9/56)]$, $2/(\lambda-1)$ for $[\mp\alpha_c\,, \pm\beta_c]$, and $2/(\lambda(\lambda-1))$ for $[-\alpha_c\,, \gamma_c(3/4)]$.

Computation for Example 3.3 with $q = 3$ and for Example 6.1: Pulling back edges towards β_c gives the following matching conditions:

$$\begin{aligned} c_n &: \lambda^3 = 2 + \frac{2}{\lambda} + \frac{2}{\lambda^2} + \ldots + \frac{2}{\lambda^{n-4}} + \frac{1}{\lambda^{n-3}} \\ a_n &: \lambda = \frac{2}{\lambda^2} + \ldots + \frac{2}{\lambda^{n-1}} \\ b_n &: \lambda = \frac{2}{\lambda^2} + \ldots + \frac{2}{\lambda^{n-2}} + \frac{2}{\lambda^{n-1}(\lambda-1)} \end{aligned}$$

Computation for Example 6.3: For the β-type Misiurewicz parameter $c = b_n$ consider the edges between α_c and $f_c(c)$. Each edge is mapped to the adjacent one by $f_c^2(z)$, as is the corresponding branch. The matching condition is

$$\lambda^2 = \frac{2}{\lambda} + \frac{2}{\lambda^3} + \ldots + \frac{2}{\lambda^{n-1}} + \frac{2}{\lambda^{n-1}(\lambda-1)}\,.$$

Computation for Example 6.5: The Hubbard tree for c_n , a_n , or b_n contains a sequence of small edges scaled by λ^4, since they are mapped to the next one by $f_c^4(z)$. The matching condition for b_n is

$$\lambda = \frac{2}{\lambda^2} + \frac{2}{\lambda^6} + \ldots + \frac{2}{\lambda^{n-2}} + \frac{2}{\lambda^{n-1}(\lambda-1)}\,.$$

B Piecewise-linear models and Galois conjugates

Suppose $c \in \mathscr{M} \cap \mathbb{R}$ and $h(c) = \log\lambda$ with $\lambda > 1$. Then $f_c(z) = z^2 + c$ is semi-conjugate to a piecewise-linear map with slope $\pm\lambda$, which can be normalized to $g_\lambda(x) = \lambda|x| - 1$ [38, 17]. If c is primitive renormalizable, the small Julia sets are squeezed to points by the semi-conjugation. Given $\lambda > 1$, we may iterate $g_\lambda^n(0)$ to obtain a kneading sequence and an external angle; in the postcritically finite case, the Hubbard tree is obtained as well, and the parameter c is found from the real or complex Spider Algorithm [26, 12].

In our real case, the external angle θ and the kneading sequence ν are easily converted: an entry A in ν means that a binary digit of θ is changing. From the kneading sequence, $g_\lambda^n(0)$ is obtained as a polynomial of degree $n-1$ in λ, which has coefficients ±1. Here $\lambda|x| - 1$ is replaced with $\pm\lambda x - 1$ according to the corresponding entry in ν. If θ is rational, or ν is preperiodic or $*$-periodic, λ is obtained from a polynomial equation. The polynomial has coefficients ±1 in the periodic case, and the lower coefficients are $\pm2, 0$ in the preperiodic case. For rational and irrational angles θ, the kneading determinant $D_c(t) = \sum_{n=0}^{\infty} \pm t^n$ is holomorphic for $t \in \mathbb{D}$; its coefficients ±1 correspond to the binary

digits 0 and 1 of the external angle $\theta \le 1/2$ associated to the real parameter c. This function is related to the generating function of lap numbers on $[-\beta_c\,,\,\beta_c]$ as follows [38]:

$$L_c(t) = \sum_{n=1}^{\infty} L(f_c^n)\, t^{n-1} = \frac{1}{1-t} + \frac{1}{(1-t)^2 D_c(t)}\,. \tag{15}$$

Now $L_c(t)$ is meromorphic in $\mathbb{D}$ and $\log L(f_c^n)$ grows as $n \log\lambda$. Thus the smallest pole of $L_c(t)$ and the smallest root of $D_c(t)$ are located at $t = 1/\lambda$. These functions are rational, if and only if the dynamics is postcritically finite, hyperbolic, or parabolic. In the p-periodic case we have $D_c(t) = P(t)\,/\,(1-t^p)$ with $P(t)$ of degree $p-1$, and the Douady substitution for any $\widehat{c} \in \mathscr{M} \cap \mathbb{R}$, and for period doubling in particular, reads

$$D_c(t) = \frac{P(t)}{1-t^p} \quad \Rightarrow \quad D_{c*\widehat{c}}(t) = P(t)\, D_{\widehat{c}}(t^p) \quad \text{and} \quad D_{c*(-1)}(t) = D_c(t)\,\frac{1-t^p}{1+t^p}\,. \tag{16}$$

Note that this gives the maximum relation of Lemma 3.9.2 for every real parameter $\widehat{c}$. Now $D_c(t)$ is constant for parameters c between a center and each of the neighboring parabolic parameters, and the satellite bifurcation changes it discontinuously at the center. But the roots of $D_c(t)$ in $\mathbb{D}$ depend continuously on c, and $h(c)$ is continuous in particular [38]: if a parameter is not hyperbolic or parabolic, it is approximated by parameters from both sides such that the first N coefficients of $D_c(t)$ are constant and $N \to \infty$. The same applies to a primitive parabolic parameter approximated from below, and the explicit change at a center does not affect roots in $\mathbb{D}$. Alternatively, Douady [17] shows that $h(c)$ cannot have a jump discontinuity: for any $1 < \lambda \le 2$, the kneading sequence of the tent map $g_\lambda(x)$ is realized in any full family of unimodal maps. Thus the monotonic map $h(c)$ is surjective, hence continuous.

For a postcritically finite real polynomial with the topological entropy $h = \log\lambda$, λ is the highest eigenvalue of a non-negative integer matrix, so it is an algebraic integer and its Galois conjugates are bounded by λ in modulus. Conversely, given $\lambda > 1$ with this property, Thurston [58, 59] constructs a postcritically finite real polynomial with the topological entropy $h = \log\lambda$. This polynomial will not be quadratic in general. For a postcritically finite real quadratic polynomial, the Galois conjugates of λ must belong to the set $\mathscr{M}_2$ defined below, which is related to an iterated function system: for complex λ with $|\lambda| > 1$ consider the holomorphic affine maps

$$g_{\lambda,\pm}(z) = \pm\lambda z - 1 \qquad g_{\lambda,\pm}^{-1}(z) = \pm\frac{1}{\lambda}(z+1) \qquad g_\lambda^{-1}(K) = g_{\lambda,+}^{-1}(K) \cup g_{\lambda,-}^{-1}(K)\,. \tag{17}$$

The corresponding attractor $\mathscr{K}_\lambda$ is non-empty and compact; according to Hutchinson [27] it is the unique compact set with $g_\lambda^{-1}(K) = K$. It is obtained as the intersection of iterated preimages of a large disk as well, so $0 \in \mathscr{K}_\lambda$ implies that the two preimages according to (17) are never disjoint, and $\mathscr{K}_\lambda$ will be connected. But $\mathscr{K}_\lambda$ may be connected also for parameters λ with $0 \notin \mathscr{K}_\lambda$; then it cannot be full.

Proposition B.1 (Barnsley–Bousch IFS and Thurston set)
Consider the compact sets $\mathscr{M}_2 \subset \mathscr{M}_1 \subset \mathscr{M}_0$ from Figure 8, which are defined by taking the closure of roots of families of polynomials, $\mathscr{M}_i = \overline{\{P^{-1}(0)\,|\,P(\lambda)\ \text{as follows}\}}$:
For the Barnsley connectedness locus $\mathscr{M}_0$, $P(\lambda)$ has coefficients $\pm1, 0$ with $P(0) \ne 0$.
For the Bousch set $\mathscr{M}_1$, $P(\lambda)$ has coefficients ±1 from any composition $g_{\lambda,\pm}^n(0)$.

For the Thurston set $\mathscr{M}_2$, $P(\lambda)$ has coefficients ± 1 from a composition $g^n_{\lambda,\pm}(0)$ corresponding to a real periodic kneading sequence.

1. *For $|\lambda|>1$ consider the Hutchinson set $\mathscr{K}_\lambda$ of the IFS (17). It is connected if and only if $\lambda \in \mathscr{M}_0$. We have $0 \in \mathscr{K}_\lambda$ if and only if $\lambda \in \mathscr{M}_1$.*

2. *$\mathscr{M}_0$ and $\mathscr{M}_1$ are invariant under inversion and under taking the n-th root. Denoting a symmetric annulus by $\mathscr{A}_r = \overline{\mathbb{D}_r} \setminus \mathbb{D}_{1/r}$, we have $\mathscr{A}_{\sqrt{2}} \subset \mathscr{M}_0 \subset \mathscr{A}_2$ and $\mathscr{A}_{\sqrt[4]{2}} \subset \mathscr{M}_1$.*

3. *$\mathscr{M}_0$ and $\mathscr{M}_1$ are locally connected and connected by Hölder paths.*

4. *$\mathscr{M}_2$ is locally connected and for $|\lambda|<1$, the sets $\mathscr{M}_2$ and $\mathscr{M}_1$ agree. Moreover, $\mathscr{M}_2$ is the closure of the set of Galois conjugates for $e^{h(c)}$, when all real centers c are considered.*

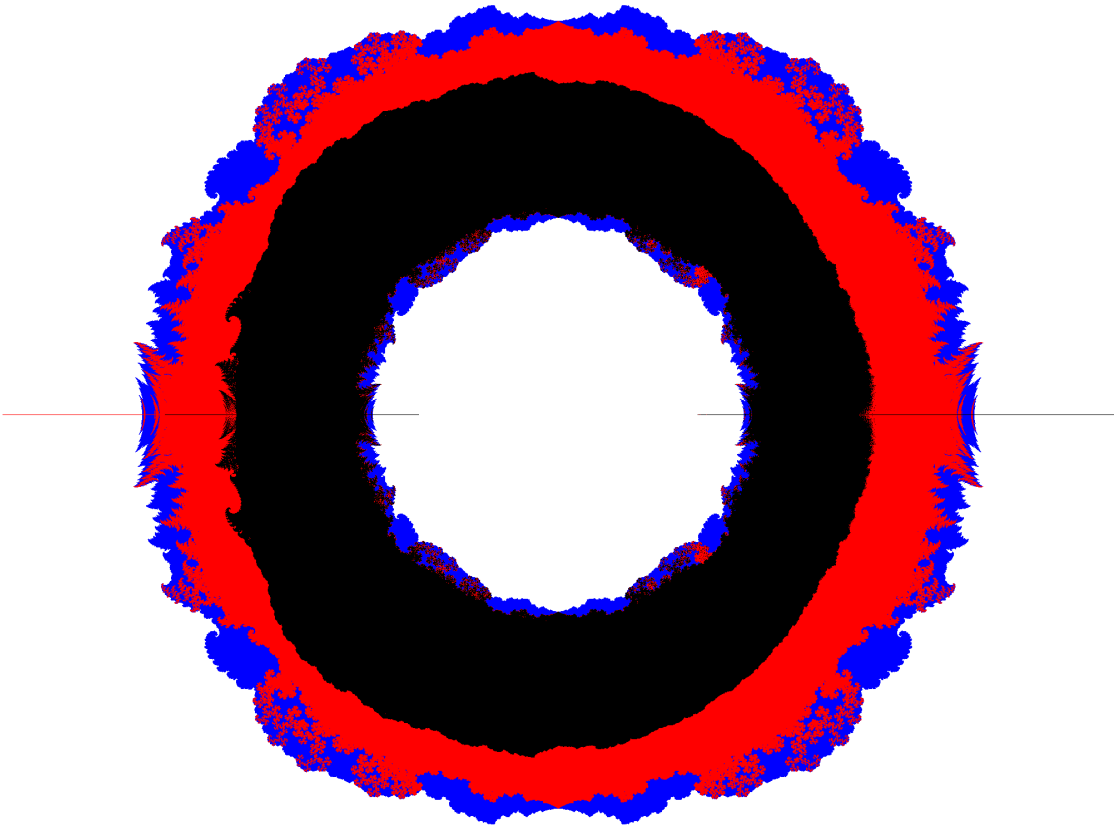

Figure 8: The sets $\mathscr{M}_2 \subset \mathscr{M}_1 \subset \mathscr{M}_0$ of Proposition B.1 are shown in black, red (light gray), and blue (dark gray), respectively [58]. The computation is based on polynomials of degree ≤ 32. Due to this restriction, $\mathscr{M}_2$ looks thinner than $\mathscr{M}_1$ for $|\lambda|<1$, but they are equal there in fact.

See [6, 7, 61] for the **proof**. Note that Bousch is using different dynamics, which are conjugate to $\frac{1}{\lambda}(z\pm 1)$ instead of $\pm\frac{1}{\lambda}(z+1)$, but the attractor $\mathscr{K}_\lambda$ will be the same due to its symmetry. For item 1, the points in $\mathscr{K}_\lambda$ are parametrized by sequences of signs as $z=\sum \pm\lambda^{-n}$, and the intersection $g^{-1}_{\lambda,+}(\mathscr{K}_\lambda) \cap g^{-1}_{\lambda,-}(\mathscr{K}_\lambda) \subset \mathscr{K}_\lambda$ is considered: $\mathscr{K}_\lambda$ is connected if the intersection is not empty. If $P(\lambda)=0$ for a polynomial with coefficients ± 1, $z=0$ will be periodic under g^{-1}_λ, so $0 \in \mathscr{K}_\lambda$. Moreover, there are parameters $\lambda \in \partial\mathscr{M}_0 \cap \partial\mathscr{M}_1$, such that the intersection is $\{0\}$ and the dynamics on $\mathscr{K}_\lambda$ is quasi-

conformally equivalent to a quadratic polynomial on a dendrite Julia set [5, 18], cf. Remark 3.10.3. See [3] for more detailed pictures of $\mathscr{M}_1$ and for the similarity between $\mathscr{M}_1$ and $\mathscr{K}_\lambda$ for suitable λ.

Due to renormalization, $\mathscr{M}_2$ is invariant under an n-th root as well. In Figure 8, $\mathscr{M}_2$ is restricted strongly for $|\lambda| > 1$, and this is interpreted as follows: for $\lambda > \sqrt{2}$ and a postcritically finite $f_c(z)$ with core entropy $h(c) = \log\lambda$, the Galois conjugates of λ are considerably smaller than λ [58, 59]. Now $\mathscr{M}_2$ is pathwise connected as well: for $|\lambda| > 1$ consider the parametrization $\mathscr{M}_2 \setminus \overline{\mathbb{D}} = \{\lambda \,|\, D_c(1/\lambda) = 0, -2 \le c \le 0\}$ by the kneading determinant. All roots of $D_c(t)$ in $\mathbb{D}$ depend continuously on the parameter c by the arguments sketched above. In the case of $|\lambda| < 1$, Tiozzo [61] shows that $\mathscr{M}_2$ and $\mathscr{M}_1$ agree by constructing a suitable dense set of polynomials. Irreducible polynomials yield the statement on Galois conjugates. See [60, 61] for images of sets, which are analogous to $\mathscr{M}_2$ for other principal veins. Thurston has started a description of quadratic and higher parameter spaces in terms of critical portraits as well, see [21, 22].

References

[1] L. Alsedà, N. Fagella, Dynamics on Hubbard trees, Fund. Math. **164**, 115–141 (2000).

[2] L. Alsedà, J. Llibre, M. Misiurewicz, *Combinatorial dynamics and entropy in dimension one*, Advanced Series in Nonlinear Dynamics **5**, World Scientific 2000.

[3] J. C. Baez, The beauty of roots, slides and blog entry (2011).
https://johncarlosbaez.wordpress.com/2011/12/11/the-beauty-of-roots/

[4] M. Baillif, A. de Carvalho, Piecewise linear model for tree maps, Internat. J. Bifur. Chaos Appl. Sci. Engineering. **11**, 3163–3169 (2001).

[5] C. Bandt, On the Mandelbrot set for pairs of linear maps, Nonlinearity **15**, 1127–1147 (2002).

[6] M. F. Barnsley, A. N. Harrington, A Mandelbrot set for a pair of linear maps, Physica **15 D**, 421–432 (1985).

[7] T. Bousch, Connexité locale et par chemins hölderiens pour les systèmes itérés de fonctions, unpublished manuscript (1993). Available from topo.math.u-psud.fr/∼bousch/preprints/ .

[8] R. Bowen, Entropy for group endomorphisms and homogeneous spaces, Trans. AMS **153**, 401–414 (1971).

[9] B. Branner, A. Douady, Surgery on complex polynomials, in: *Holomorphic dynamics*, X. Gomez-Mont et al. eds., LNM **1345**, Springer 1988, 11–72.

[10] H. Bruin, D. Schleicher, *Symbolic dynamics of quadratic polynomials*, preprint of 2002. https://www.mittag-leffler.se/preprints/

[11] H. Bruin, D. Schleicher, Hausdorff dimension of biaccessible angles for quadratic polynomials, preprint (2012). arXiv:1205.2544

[12] X. Buff, Cui G.-Zh., Tan L., Teichmüller spaces and holomorphic dynamics, in: *Handbook of Teichmüller theory, Vol. IV*, A. Papadopoulos ed., Soc. math. europ., to appear. Preprint of 2011.

[13] S. Bullett, P. Sentenac, Ordered orbits of the shift, square roots, and the devil's staircase, Math. Proc. Camb. Phil. Soc. **115**, 451–481 (1994).

[14] A. Douady, J. H. Hubbard, On the dynamics of polynomial-like mappings, Ann. Sci. École Norm. Sup. **18**, 287–343 (1985).

[15] A. Douady, Algorithms for computing angles in the Mandelbrot set, in: *Chaotic Dynamics and Fractals*, M. F. Barnsley, S. G. Demko eds., Notes Rep. Math. Sci. Eng. **2**, 155–168 (1986).

[16] A. Douady, Descriptions of compact sets in $\mathbb{C}$, in: *Topological methods in modern mathematics*, L. R. Goldberg ed., Publish or Perish 1993, 429–465.

[17] A. Douady, Topological entropy of unimodal maps: monotonicity for quadratic polynomials, in: *Real and complex dynamical systems* (Hillerød 1993), NATO Adv. Sci. Inst. Ser. C Math. Phys. Sci. **464**, Kluwer 1995, 65–87.

[18] K. E. Eroğlu, S. Rohde, B. Solomyak, Quasisymmetric conjugacy between quadratic dynamics and iterated function systems, Ergod. Th. Dynam. Sys. **30**, 1665–1684 (2010). arXiv:0806.3952

[19] K. Falconer, *Fractal geometry, mathematical foundations and applications*, Wiley 2003.

[20] H. Furstenberg, Disjointness in ergodic theory, minimal sets, and a problem in Diophantine approximation, Math. Systems Theory **1**, 1–49 (1967).

[21] Gao Y., Tan L., On Bill Thurston's binding entropy theory, Presentation in Holbæk 2012.

[22] Gao Y., *Dynatomic periodic curve and core entropy for polynomials*, Ph.D. thesis Angers University and Chinese Academy of Science 2013.
Available from http://hal.archives-ouvertes.fr.

[23] J. Graczyk, G. Swiątek, Generic hyperbolicity in the logistic family, Ann. Math. **146**, 1–56 (1997).

[24] R. A. Horn, C. R. Johnson, *Matrix analysis*, Cambridge University Press 1985.

[25] J. H. Hubbard, Local connectivity of Julia sets and bifurcation loci: Three theorems of J.-C. Yoccoz, in: *Topological methods in modern mathematics*, L. R. Goldberg ed., Publish or Perish 1993, 467–511, 375–378.

[26] J. H. Hubbard, D. Schleicher, The Spider Algorithm, in: *Complex Dynamical Systems*, R. L. Devaney ed., Proc. Symp. Appl. Math. **49**, AMS 1994, 155–180.

[27] J. E. Hutchinson, Fractals and self similarity, Indiana Univ. Math. J. **30**, 713–747 (1981).

[28] W. Jung, Renormalization and embedded Julia sets in the Mandelbrot set, preprint in preparation (2014).

[29] W. Jung, Self-similarity and homeomorphisms of the Mandelbrot set, preprint in preparation (2014).

[30] G. M. Levin, S. van Strien, Local connectivity of the Julia set of real polynomials, Ann. Math. **147**, 471–541 (1998).

[31] T. Li, *A monotonicity conjecture for the entropy of Hubbard trees*, Ph.D. thesis SUNY Stony Brook 2007. Available from www.math.sunysb.edu/dynamics/theses.

[32] J. Llibre, M. Misiurewicz, Horseshoes, entropy and periods for graph maps, Topology **32**, 649–664 (1993).

[33] M. Lyubich, Dynamics of quadratic polynomials, I-II, Acta Math. **178**, 185–297 (1997).

[34] A. Manning, Logarithmic capacity and renormalizability for landing on the Mandelbrot set, Bull. London Math. Soc. **28**, 521–526 (1996).

[35] C. T. McMullen, *Complex Dynamics and Renormalization*, Annals of Mathematics Studies **135**, Princeton University Press 1995.

[36] Ph. Meerkamp, D. Schleicher, Hausdorff dimension and biaccessibility for polynomial Julia sets, Proc. Amer. Math. Soc. **141**, 533–542 (2013). arXiv:1101.4702

[37] W. de Melo, S. van Strien, *One-dimensional dynamics*, Springer 1993.

[38] J. Milnor, W. Thurston, On iterated maps of the interval, in: *Dynamical Systems*, J. C. Alexander ed., LNM **1342**, Springer 1988, 465–563.

[39] J. Milnor, Local connectivity of Julia sets: Expository lectures, in: *The Mandelbrot Set, Theme and Variations*, Tan L. ed., LMS Lecture Notes **274**, Cambridge University Press 2000, 67–116. arxiv:math/9207220

[40] J. Milnor, Periodic Orbits, External Rays and the Mandelbrot Set: An Expository Account, Astérisque **261**, 277–333 (2000). arxiv:math/9905169

[41] J. Milnor, Tsujii's Monotonicity Proof for Real Quadratic Maps, unpublished manuscript (2000).

[42] M. Misiurewicz, W. Szlenk, Entropy of piecewise monotone mappings, Studia Math. **67**, 45–63 (1980).

[43] M. Misiurewicz, S. V. Shlyachkov, Entropy of piecewise continuous interval maps, in *European Conference on Iteration Theory 89*, Ch. Mira ed., World Scientific 1991, 239–245.

[44] Ch. Penrose, *On quotients of shifts associated with dendrite Julia sets of quadratic polynomials*, Ph.D. thesis University of Coventry 1994.
A related manuscript of 2000 is available from www.maths.qmul.ac.uk/∼csp/ .

[45] J. Riedl, D. Schleicher, On Crossed Renormalization of Quadratic Polynomials, in: *Proceedings of the* 1997 *conference on holomorphic dynamics*, RIMS Kokyuroku **1042**, 11–31, Kyoto 1998.

[46] J. Riedl, *Arcs in Multibrot Sets, Locally Connected Julia Sets and Their Construction by Quasiconformal Surgery*, Ph.D. thesis TU München 2000.
Available from www.math.sunysb.edu/dynamics/theses for 2001.

[47] D. Schleicher, On Fibers and Local Connectivity of Mandelbrot and Multibrot Sets, in: *Fractal geometry and applications*, Lapidus, Frankenhuysen eds., Proc. Symp. Appl. Math. **72**, AMS 2004, 477–512. arXiv:math/9902155

[48] D. Schleicher, On Fibers and Renormalization of Julia Sets and Multibrot Sets, preprint (1998). arXiv:math/9902156.

[49] D. Schleicher, Rational Parameter Rays of the Mandelbrot Set, Astérisque **261**, 405–443 (2000). arxiv:math/9711213

[50] Z. Słodkowsky, Holomorphic motions and polynomial hulls, Proc. Am. Math. Soc. **111**, 347–355 (1991).

[51] S. Smirnov, On supports of dynamical laminations and biaccessible points in polynomial Julia sets, Colloq. Math. **87**, 287–295 (2001).

[52] D. E. K. Sørensen, Accumulation theorems for quadratic polynomials, Ergod. Th. Dynam. Sys. **16**, 1–36 (1996).

[53] D. E. K. Sørensen, Infinitely renormalizable quadratic polynomials, with non-locally connected Julia set, J. Geometric Analysis **10**, 169–206 (2000).

[54] P. Štefan, A theorem of Šharkovskiĭ on the existence of periodic orbits of continuous endomorphisms of the real line, Comm. Math. Phys. **54**, 237–248 (1977).

[55] Tan L., Similarity between the Mandelbrot set and Julia sets, Comm. Math. Phys. **134**, 587–617 (1990).

[56] W. Thurston, On the geometry and dynamics of iterated rational maps, in: *Complex dynamics: families and friends*, D. Schleicher ed., AK Peters 2009, 1–137.

[57] W. Thurston, Core entropy, talk at "Holomorphic Dynamics around Thurston's Theorem", Roskilde 2010. Citation according to the Abstract.

[58] W. Thurston, Real polynomial entropy, talk at "Frontiers in Complex Dynamics", Banff 2011. Citation according to the slides and video.

[59] W. Thurston, Entropy in dimension one, preprint 2011. Edited by S. Koch, to appear.

[60] G. Tiozzo, Topological entropy of quadratic polynomials and dimension of sections of the Mandelbrot set, preprint (2013). arXiv:1305.3542

[61] G. Tiozzo, Galois conjugates of entropies of real unimodal maps, preprint (2013). arXiv:1310.7647

[62] M. Tsujii, A simple proof for monotonicity of entropy in the quadratic family, Ergodic Th. Dynam. Sys. **20**, 925–933 (2000).

[63] S. Zakeri, Biaccessibility in quadratic Julia sets, Ergod. Th. Dynam. Sys. **20**, 1859–1883 (2000).

[64] S. Zakeri, Biaccessibility in Quadratic Julia Sets II: The Siegel and Cremer Cases, preprint (1998). arXiv:math/9801150

[65] S. Zakeri, External rays and the real slice of the Mandelbrot set, Ergod. Th. Dynam. Sys. **23**, 637–660 (2003). arXiv:math/0210382

[66] S. Zakeri, On biaccessible points of the Mandelbrot set, Proc. Amer. Math. Soc. **134**, 2239–2250 (2006).

[67] Anna Zdunik, On biaccessible points in Julia sets of polynomials, Fund. Math. **163**, 277–286 (2000).

The program Mandel is available from www.mndynamics.com. For dyadic angles you can compute $B_{\text{comb}}(\theta)$ and zoom into its graph. Or display the fractals of Appendix B.